

High-Performance Two-Photon Absorption Luminophores: Large Action Cross Sections, Free from Fluorescence Quenching, and Tunable Emission of Efficient Non-Doped Organic Light-Emitting Diodes

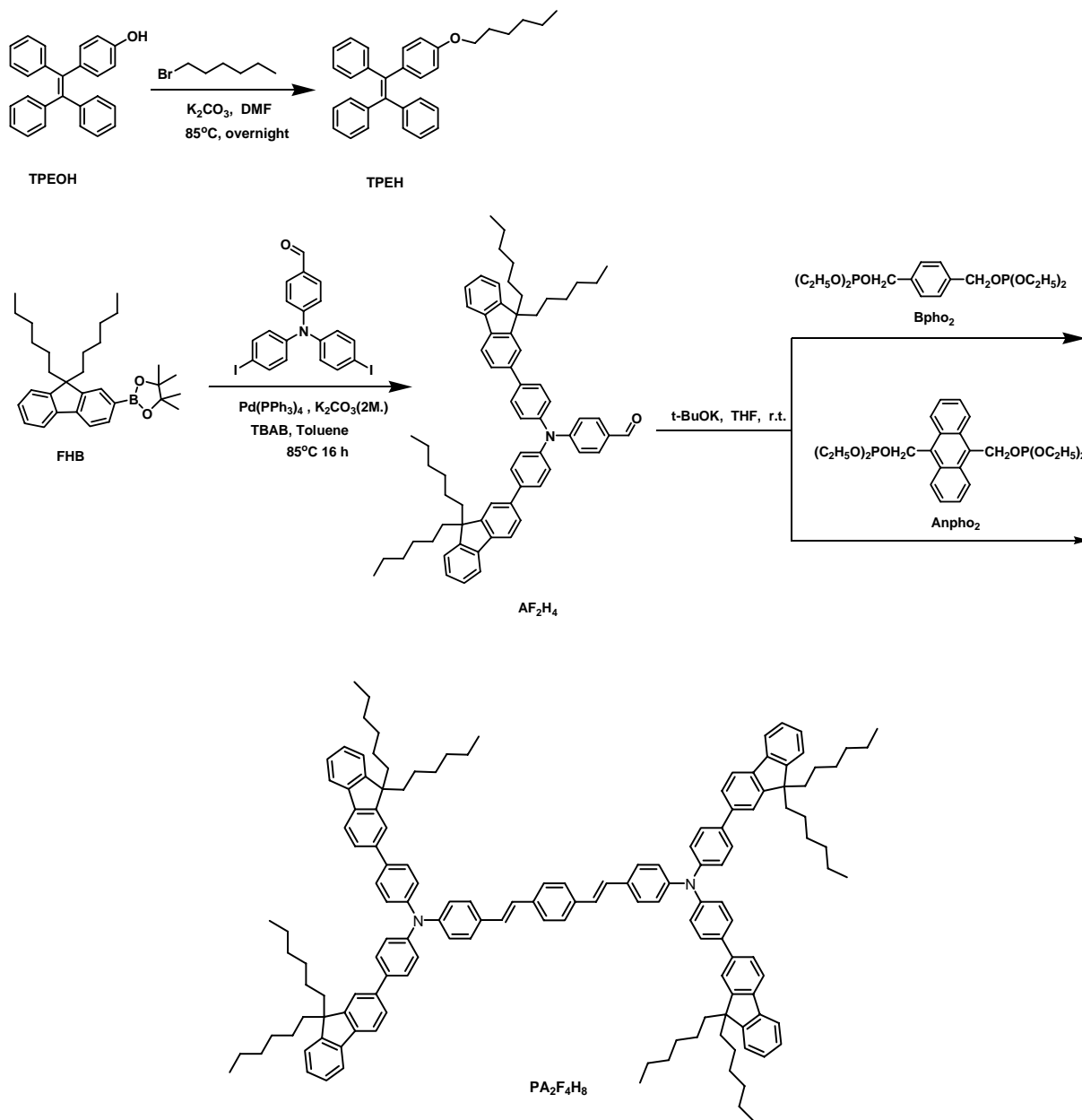
Bingjia Xu,^{‡a} Jiajun He,^{‡a} Yang Liu,^b Bin Xu,^b Qiangzhong Zhu,^c Mingyuan Xie,^c Zebo Zheng,^c Zhenguo Chi,^{*a} Wenjing Tian,^b Chongjun Jin,^c Fuli Zhao,^c and Jiarui Xu^{*a}.

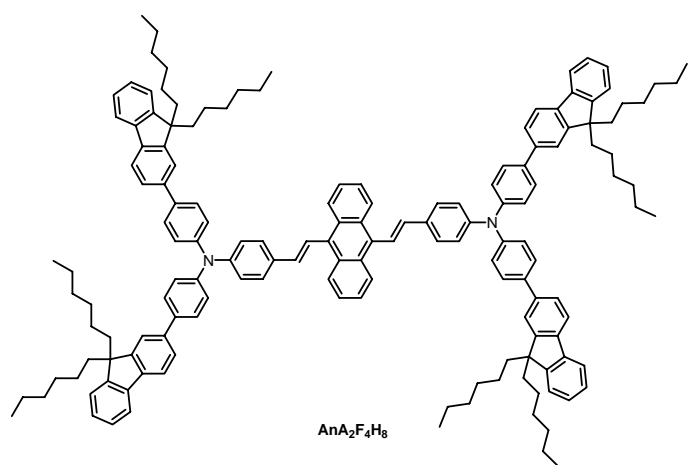
^a PCFM Lab, DSAPM Lab, KLGHEI of Environment and Energy Chemistry, State Key Laboratory of Optoelectronic Material and Technologies, School of Chemistry and Chemical Engineering, Sun Yet-sen University, Guangzhou 510275, P. R. China.

^b State Key Laboratory of Supramolecular Structure and Material, Jilin University, Changchun 130012, P. R. China

^c School of Physics and Engineering, Sun Yat-sen University, Guangzhou 510275, P.R. China.

Supporting Information





Scheme S1. Synthetic routes of PA₂F₄H₈ and AnA₂F₄H₈

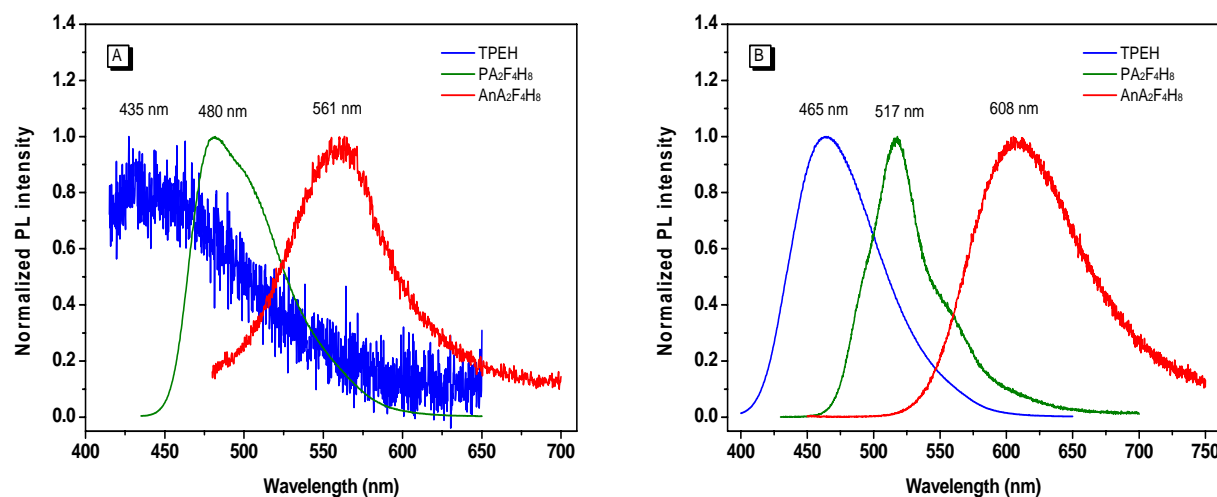


Fig. S1 PL spectra of TPEH, PA₂F₄H₈, and AnA₂F₄H₈: (A) 10 μM in THF solution; (B) at solid state.

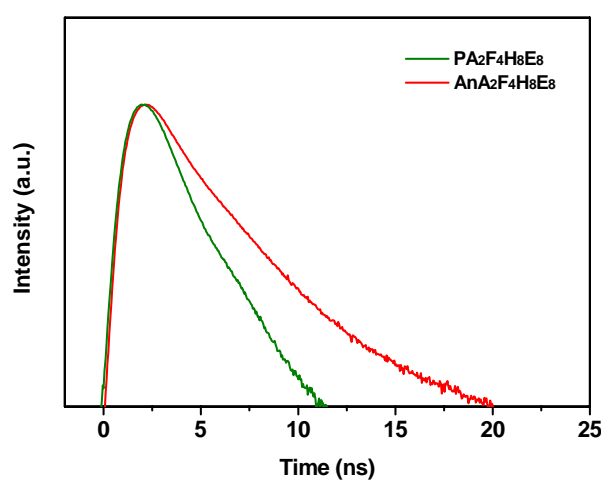


Fig. S2 Time-resolved emission decay curves of the compounds

Table S1. Fluorescence decay parameters of the compounds

Compound	PA ₂ F ₄ H ₈ E ₈	AnA ₂ F ₄ H ₈ E ₈
τ_1 (ns) ^a	0.74	0.65
A ₁ ^b	0.60	0.22
τ_2 (ns)	1.27	1.72
A ₂	0.39	0.70
τ_3 (ns)	12.22	5.30
A ₂	0.01	0.06
τ_4 (ns) ^c	N/A	27.33
A ₄	N/A	0.01
$\langle\tau\rangle$ (ns) ^c	1.04	2.05

^a Fluorescence lifetime, ^b Fractional contribution, ^c mean lifetime.

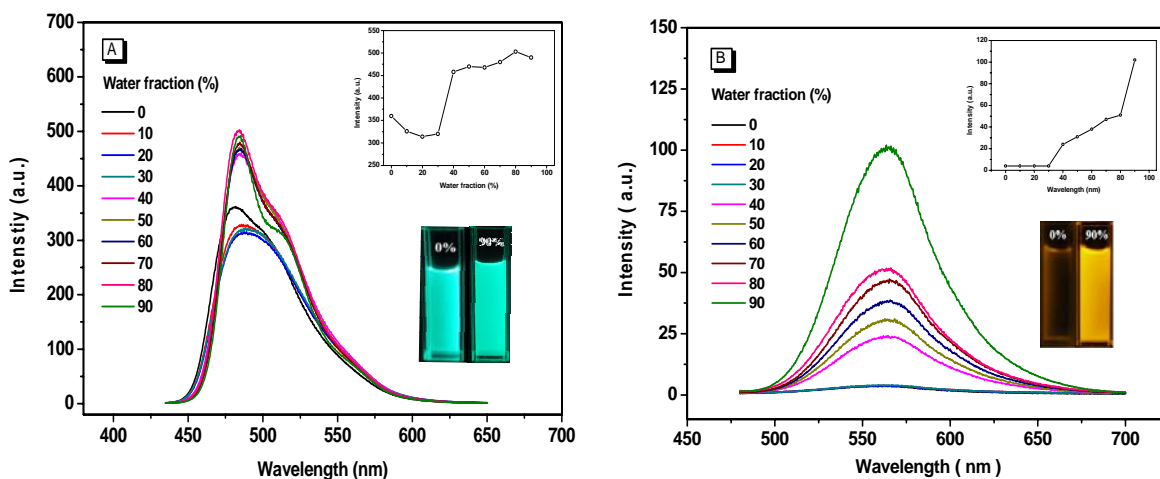
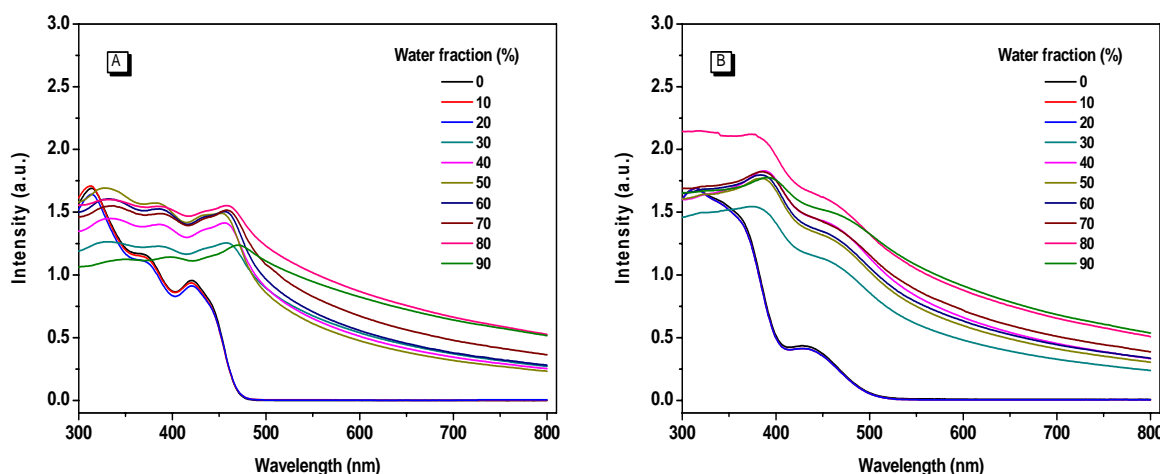


Fig. S3 PL spectra of the dilute solutions of PA₂F₄H₈ (A) and AnA₂F₄H₈ (B) in water/THF mixtures with different volume fractions of water (concentration: 10 μM). The insets depict changes in PL peak intensity (up) and emission images of the compounds in pure THF and 90% water fraction mixture under 365 nm UV illumination (10 μM) (down).



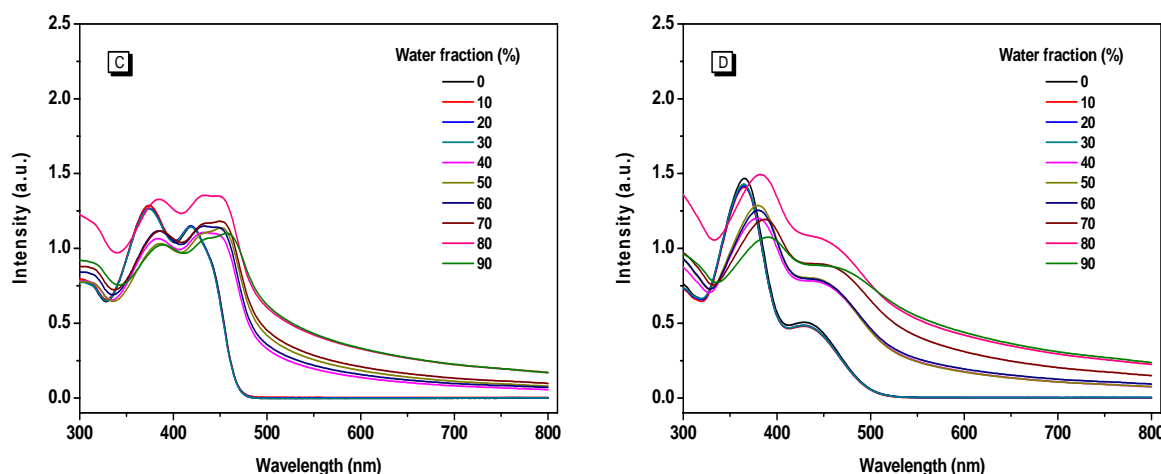


Fig. S4 UV absorption spectra of $\text{PA}_2\text{F}_4\text{H}_8\text{E}_8$ (A), $\text{AnA}_2\text{F}_4\text{H}_8\text{E}_8$ (B), $\text{PA}_2\text{F}_4\text{H}_8$ (C), and $\text{AnA}_2\text{F}_4\text{H}_8$ (D) in water/THF mixtures with different volume fractions of water (concentration: 10 μM)

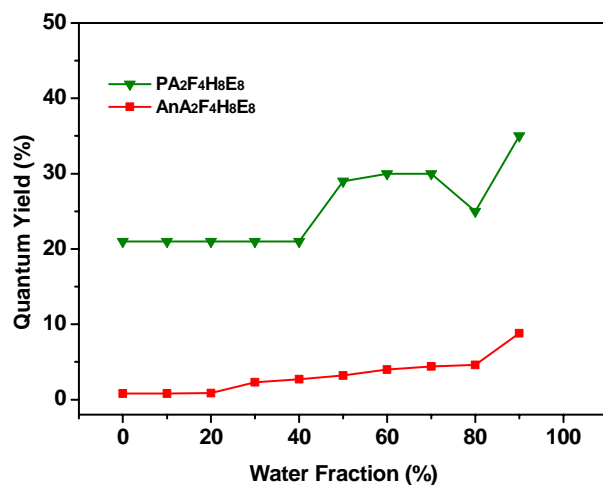


Fig. S5 The quantum yields of the compounds in water/THF mixtures (Standard: fluorescein in 0.1 N sodium hydroxide)

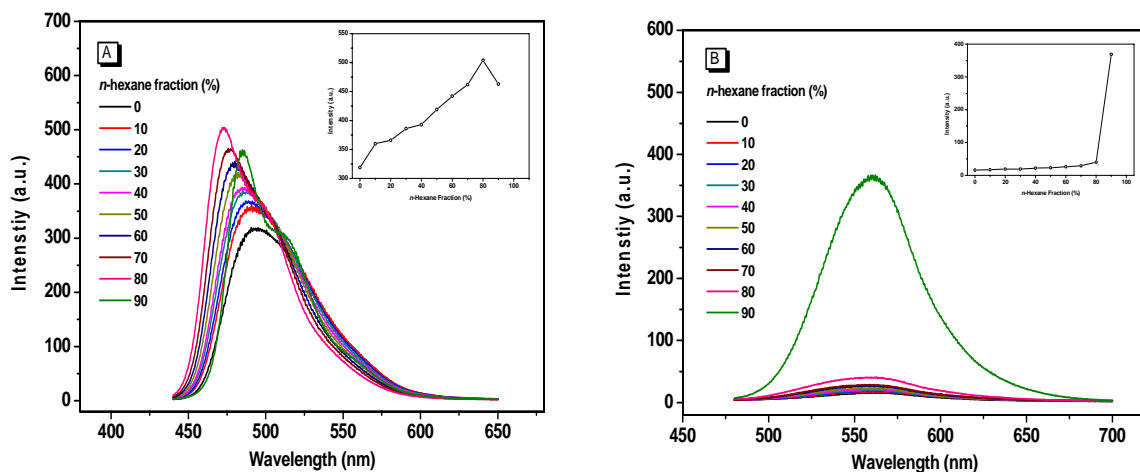


Fig. S6 PL spectra of the dilute solutions of $\text{PA}_2\text{F}_4\text{H}_8\text{E}_8$ (A) and $\text{AnA}_2\text{F}_4\text{H}_8\text{E}_8$ (B) in n -hexane/ CH_2Cl_2 mixtures with different volume fractions of n -hexane (concentration: 10 μM).

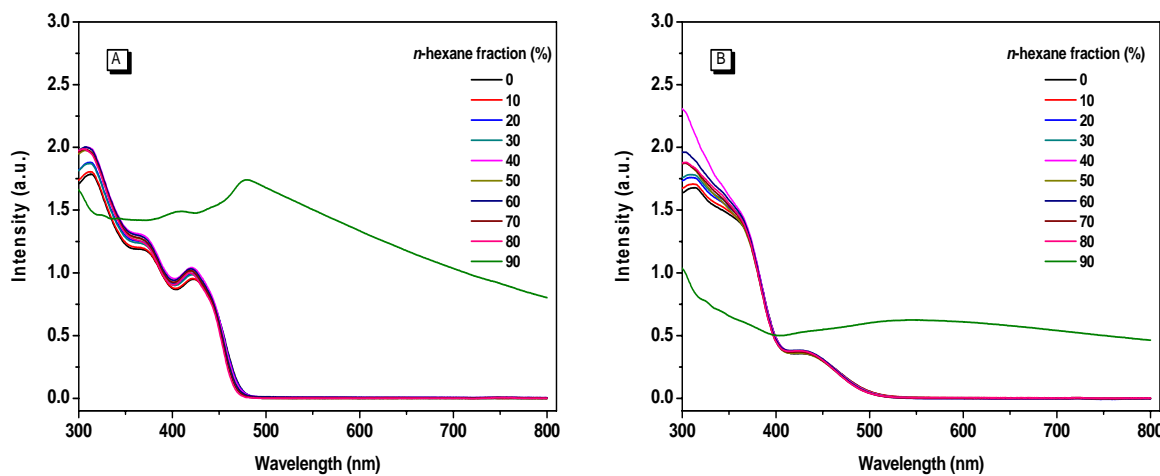


Fig. S7 UV absorption spectra of $\text{PA}_2\text{F}_4\text{H}_8\text{E}_8$ (A), $\text{AnA}_2\text{F}_4\text{H}_8\text{E}_8$ (B), $\text{PA}_2\text{F}_4\text{H}_8$ (C), and $\text{AnA}_2\text{F}_4\text{H}_8$ (D) in n -hexane/CH₂Cl₂ mixtures with different volume fractions of n -hexane (concentration: 10 μM)

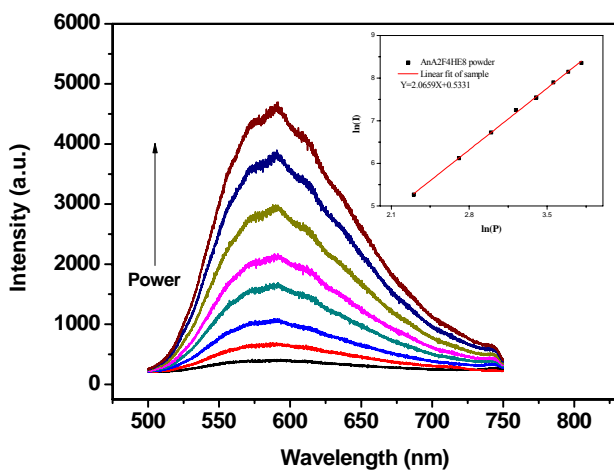


Fig. S8 Two Photon Fluorescence (TPF) emission spectra of $\text{AnA}_2\text{F}_4\text{H}_8\text{E}_8$ at solid state with different input power; the inset depicts the plot of the emission intensity versus input laser power for $\text{AnA}_2\text{F}_4\text{H}_8\text{E}_8$ on a log/log scale. The fit of the experimental data is shown in black, and the corresponding equation is reported in the inset. (The excitation was 800 nm femtosecond laser).

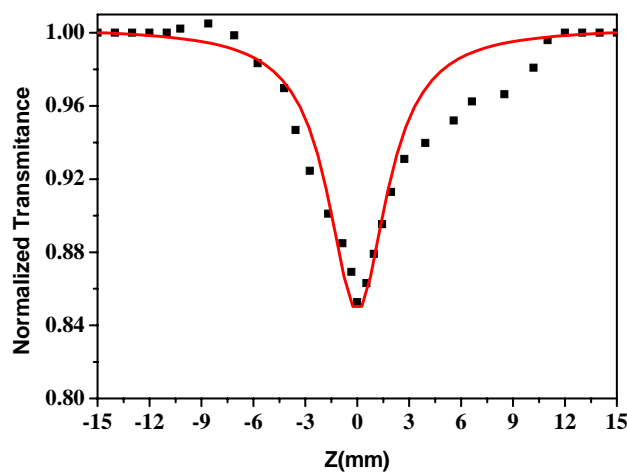


Fig. S9 Normalized Z-scan transmittance of $\text{PA}_2\text{F}_4\text{H}_8\text{E}_8$ (Using femtosecond pulse at $\lambda=800$ nm, concentration of $\text{PA}_2\text{F}_4\text{H}_8\text{E}_8$: 5 mM in THF). The solid line is the theoretical result.

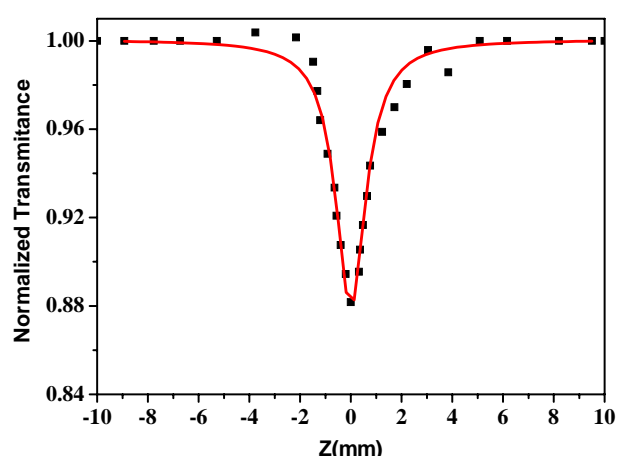


Fig. S10 Normalized Z-scan transmittance of $\text{AnA}_2\text{F}_4\text{H}_8\text{E}_8$ (Using femtosecond pulse at $\lambda=800$ nm, concentration of $\text{AnA}_2\text{F}_4\text{H}_8\text{E}_8$: 5 mM in THF). The solid line is the theoretical result.

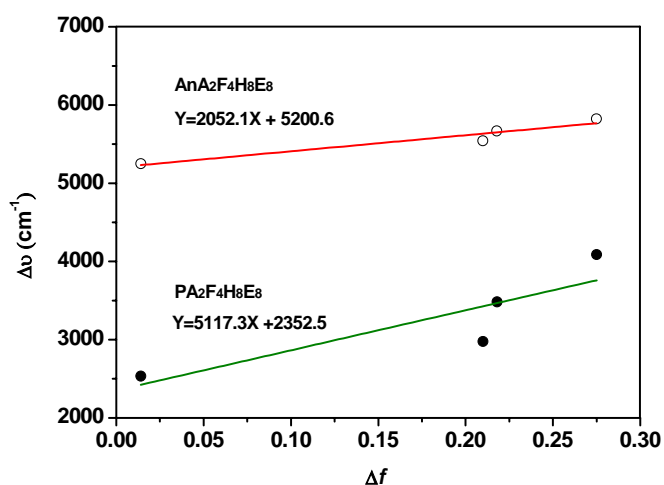


Fig. S11 Plots of Stokes shift ($\Delta\nu$) of $\text{PA}_2\text{F}_4\text{H}_8\text{E}_8$ and $\text{AnA}_2\text{F}_4\text{H}_8\text{E}_8$ vs. solvent polarity

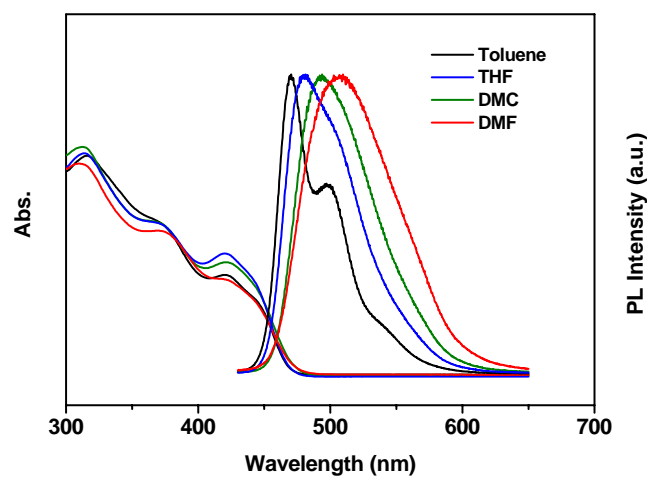


Fig. S12 UV-Visible absorption and PL spectra of $\text{PA}_2\text{F}_4\text{H}_8\text{E}_8$ in different solvents

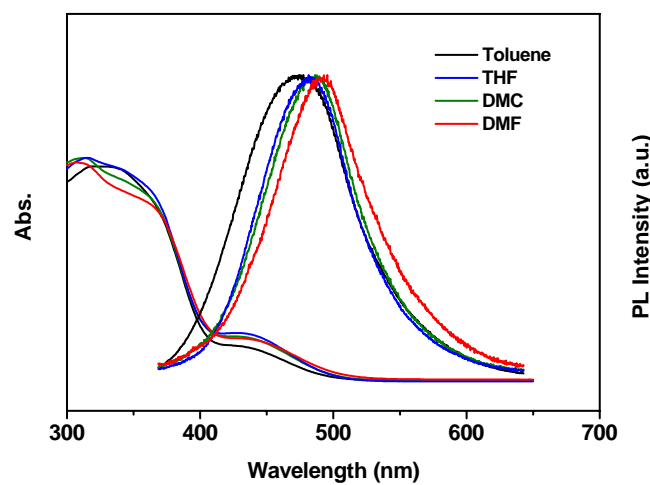


Fig. S13 UV-Visible absorption and PL spectra of $\text{AnA}_2\text{F}_4\text{H}_8\text{E}_8$ in different solvents

Table S2. Photophysical properties of the compounds in different solvents

Solvent	λ_{abs} (nm)	$\lambda_{\text{max}}^{\text{em}}$ (nm)	Δf	$\Delta \nu (\text{cm}^{-1})$
$\text{PA}_2\text{F}_4\text{H}_8\text{E}_8$				
Toluene	317; 370; 420	470	0.014	2532.9
THF	314; 370; 420	480	0.210	2976.2
DCM	312; 370; 420	492	0.218	3484.3
DMF	311; 374; 420	507	0.275	4085.7
$\text{AnA}_2\text{F}_4\text{H}_8\text{E}_8$				
Toluene	317; 360; 428	552	0.014	5248.5
THF	314; 360; 428	561	0.210	5539.2
DCM	312; 360; 428	565	0.218	5665.4
DMF	308; 365 428	570	0.275	5820.6

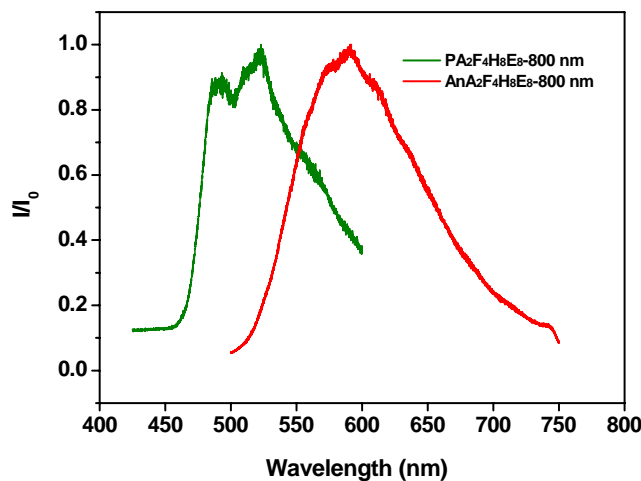


Fig. S14 Two Photon Fluorescence (TPF) emission spectra of the compounds at solid state

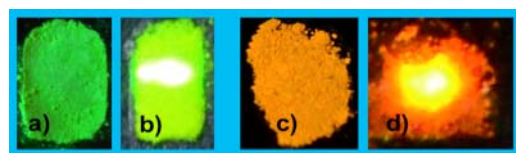


Fig. S15 Photos of one- and two-photonfluorescence emission of the compounds at solid state: a) one-photon fluorescence of PA₂F₄H₈E₈; b) two-photon fluorescence of PA₂F₄H₈E₈; c) one-photon fluorescence of AnA₂F₄H₈E₈; d) two-photon fluorescence of AnA₂F₄H₈E₈.

Table S3. Thermal and electrochemical properties of the compounds

Compounds	T _{d, 5%} (°C)	T _g (°C) ^a	T _m (°C) ^b	E _{onset} (V)	E _{p1} (V)	E _{p2} (V)	HOMO (eV)	LUMO (eV)	ΔE _g (eV)
PA ₂ F ₄ H ₈ E ₈	423	118	N/A	1.17	1.35	1.54	-5.44	-2.79	2.65
AnA ₂ F ₄ H ₈ E ₈	438	118	N/A	1.17	1.35	1.51	-5.44	-2.95	2.49

^{a,b} Obtained from second run

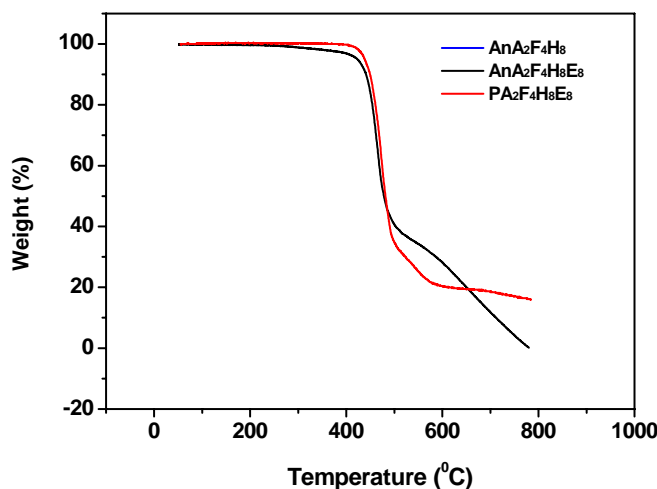


Fig. S16 TGA curves of the compounds.

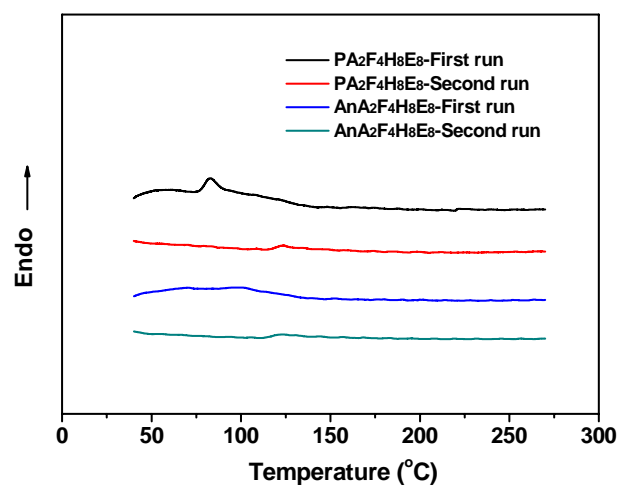


Fig. S17 DSC analysis of the compounds

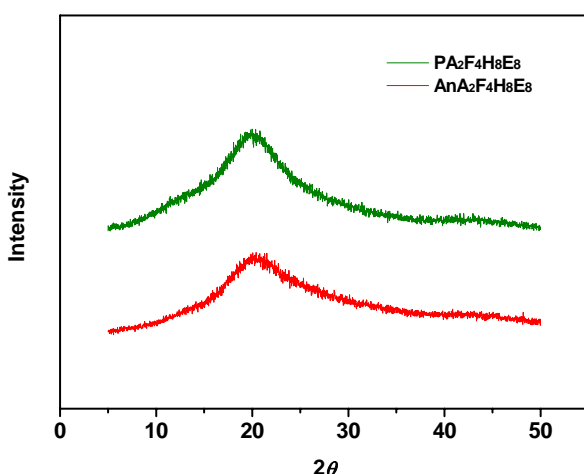


Fig. S18 The powder XRD diffraction patterns of the compounds

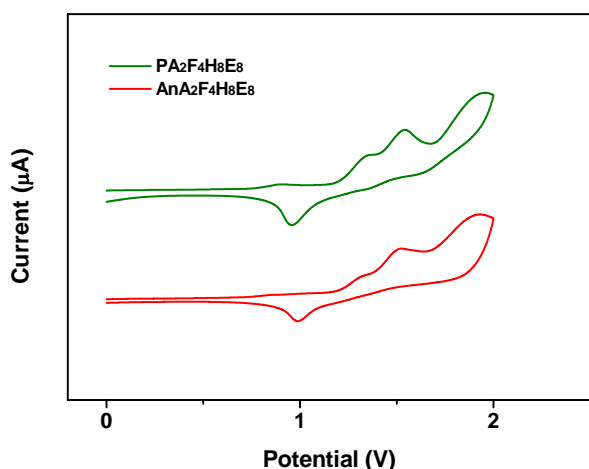


Fig. S19 Cyclic voltammetry curves of the compounds

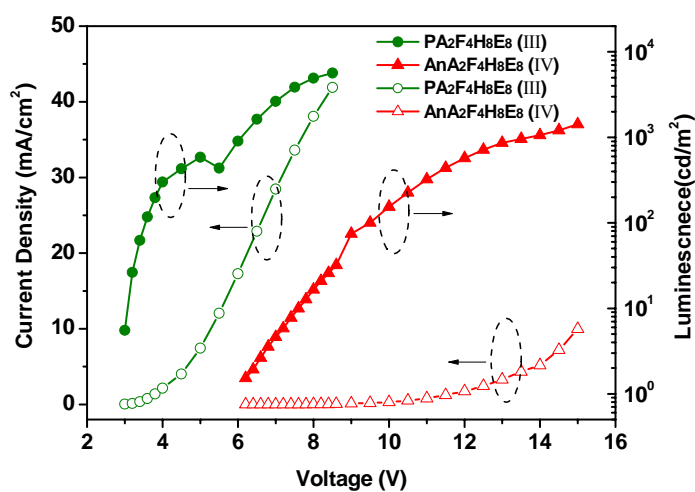


Fig. S20 Current density–voltage–luminance characteristics for the EL devices of (III) and (IV)

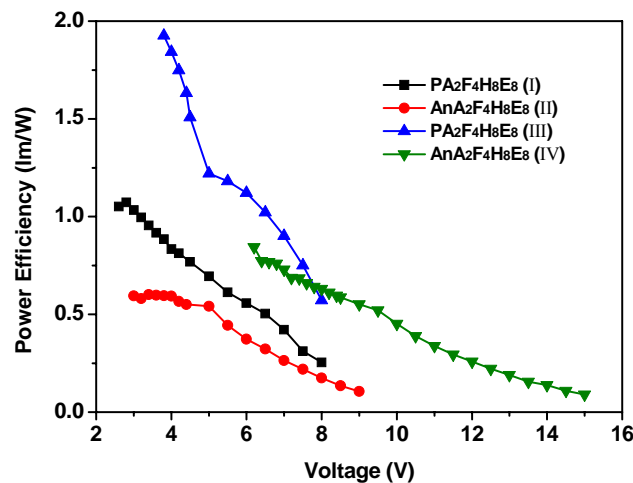


Fig. S21 Power efficiency–voltage characteristics of the EL devices

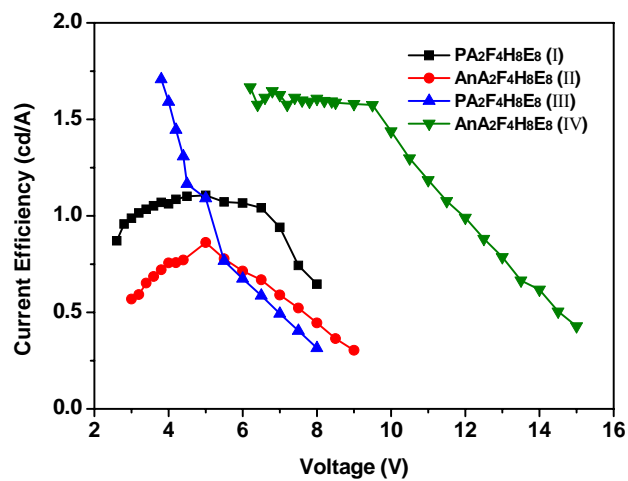
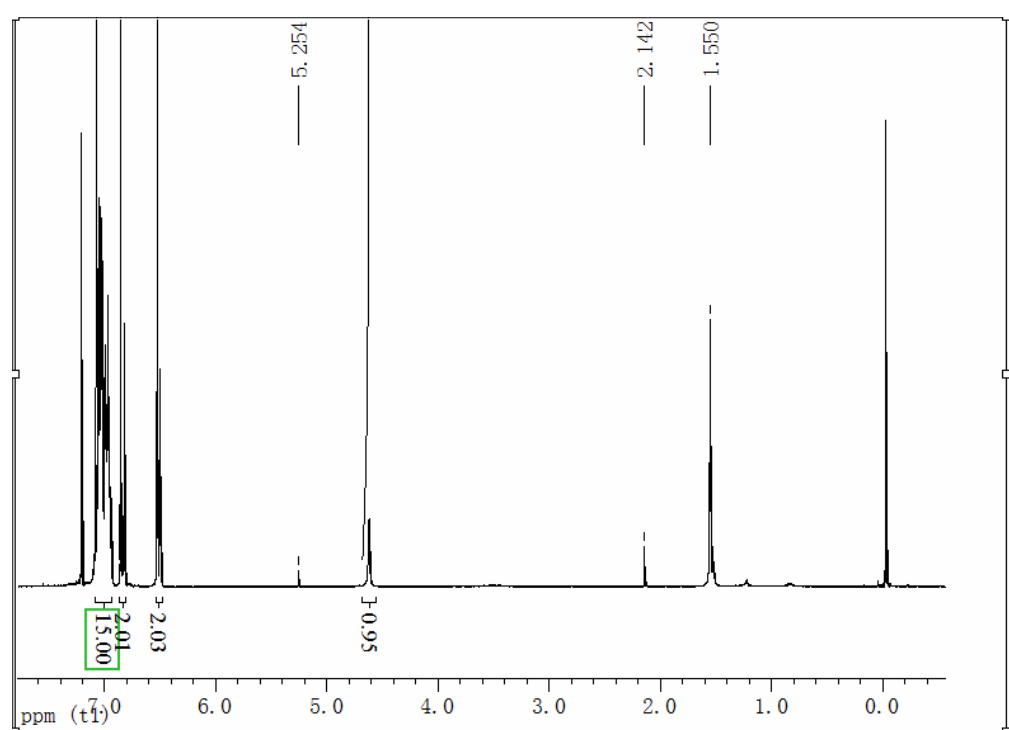


Fig. S22 Current efficiency–voltage characteristics of the EL devices

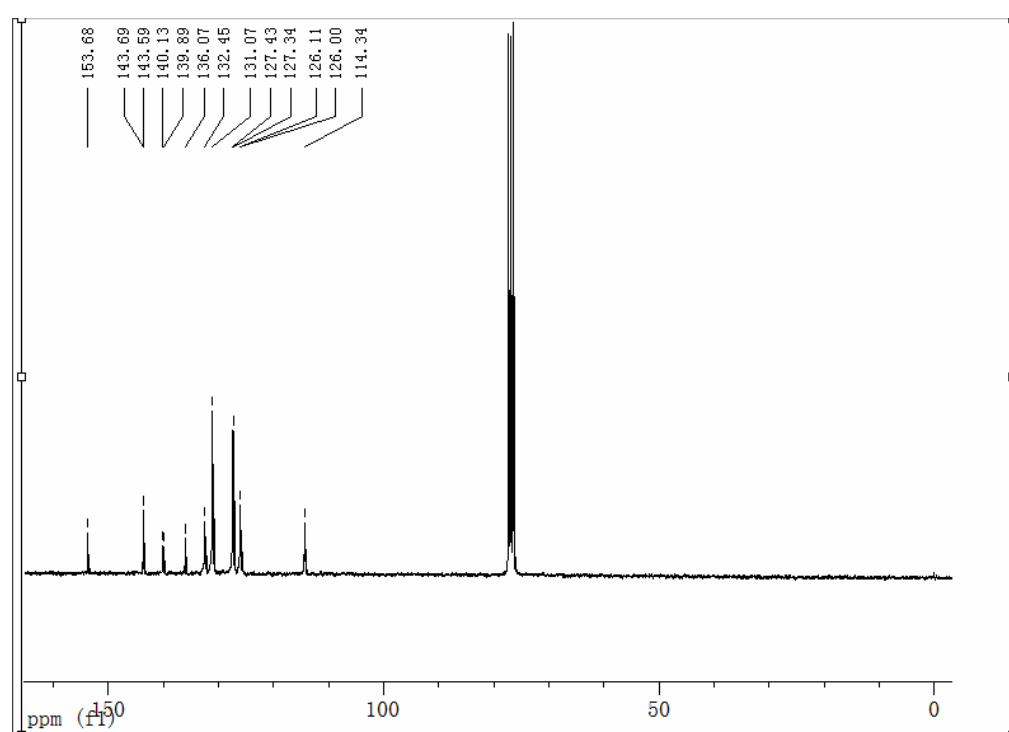
Structure Information of the Intermediate and Final products

1. TPEOH

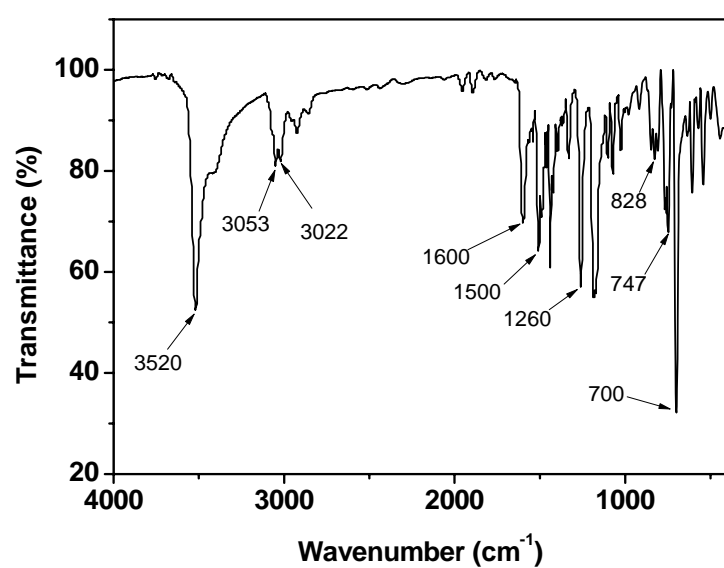
¹H NMR



¹³C NMR



FT-IR



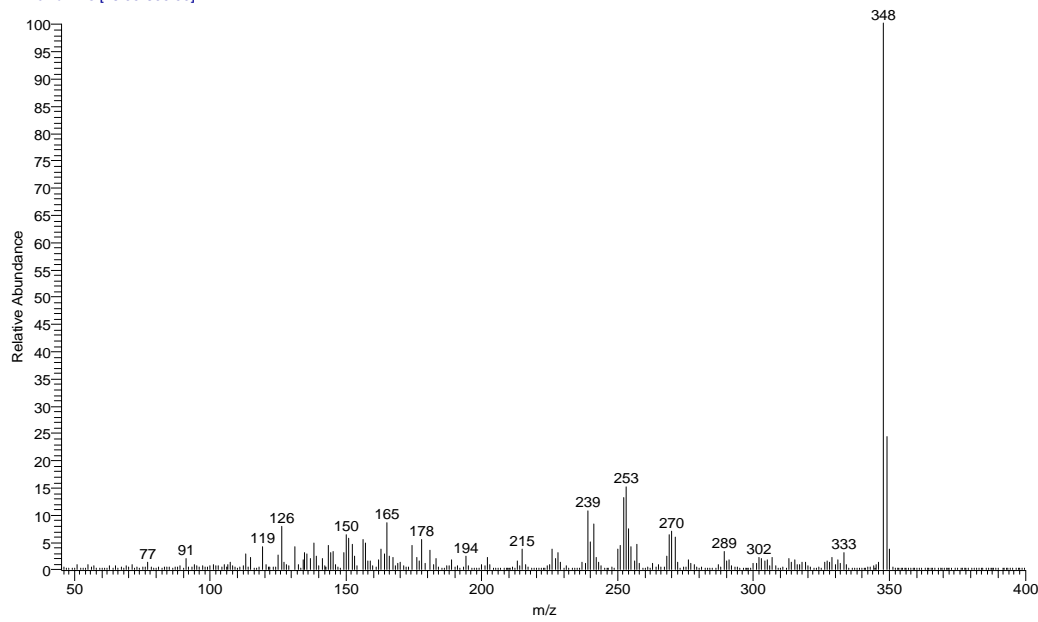
EI-MS

Instrument:DSQ(Thermo)
Ionization Method: EI
D:\DSQDATA-LR12010901

1/9/2012 10:14:26 AM

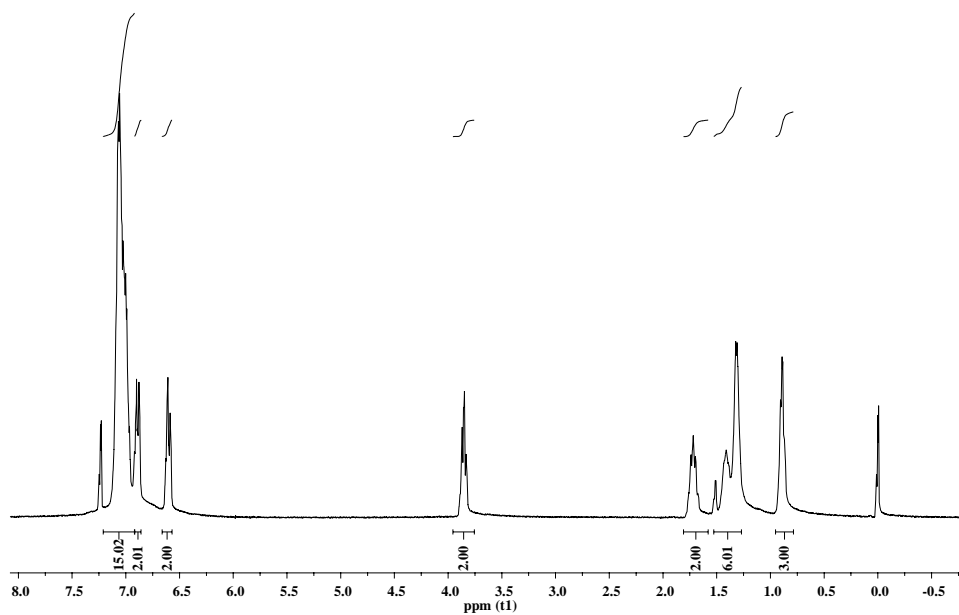
TPEOH

010901 #168 RT: 2.04 AV: 1 NL: 5.13E7
T: + c Full ms [45.00-600.00]

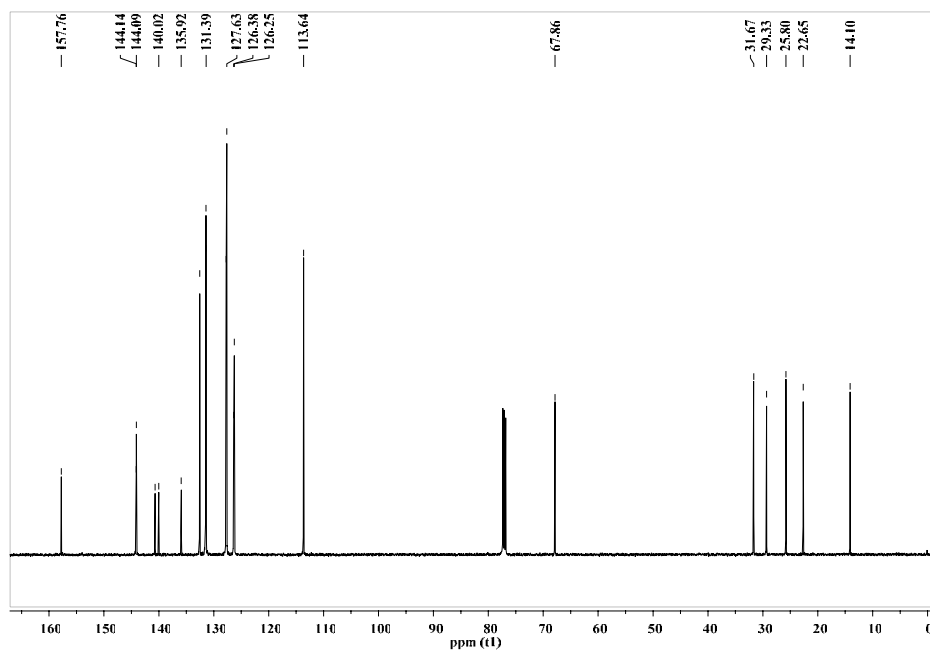


2. TPEH

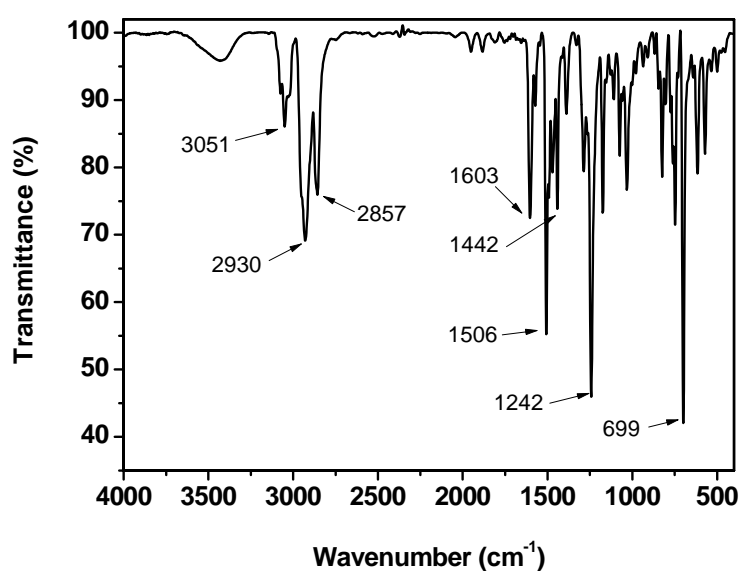
^1H NMR



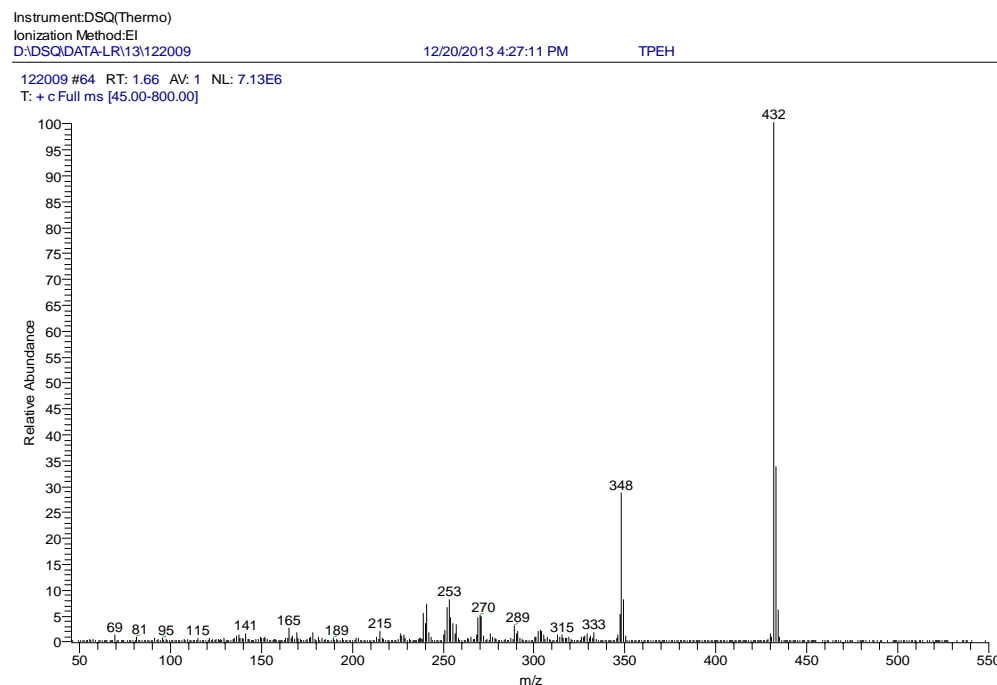
^{13}C NMR



FT-IR

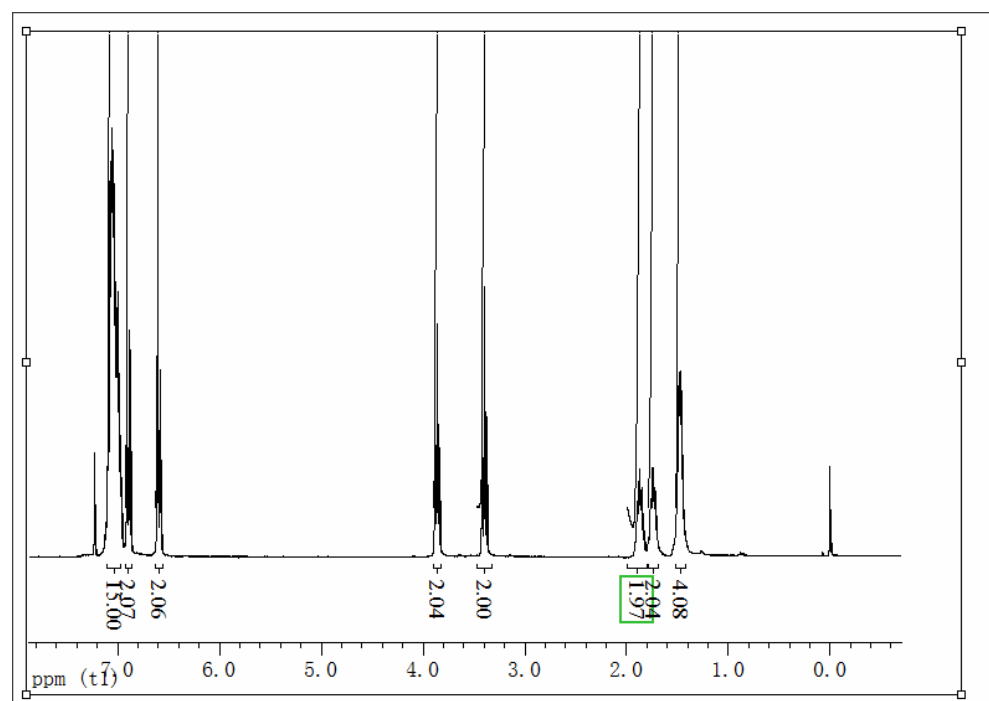


MS

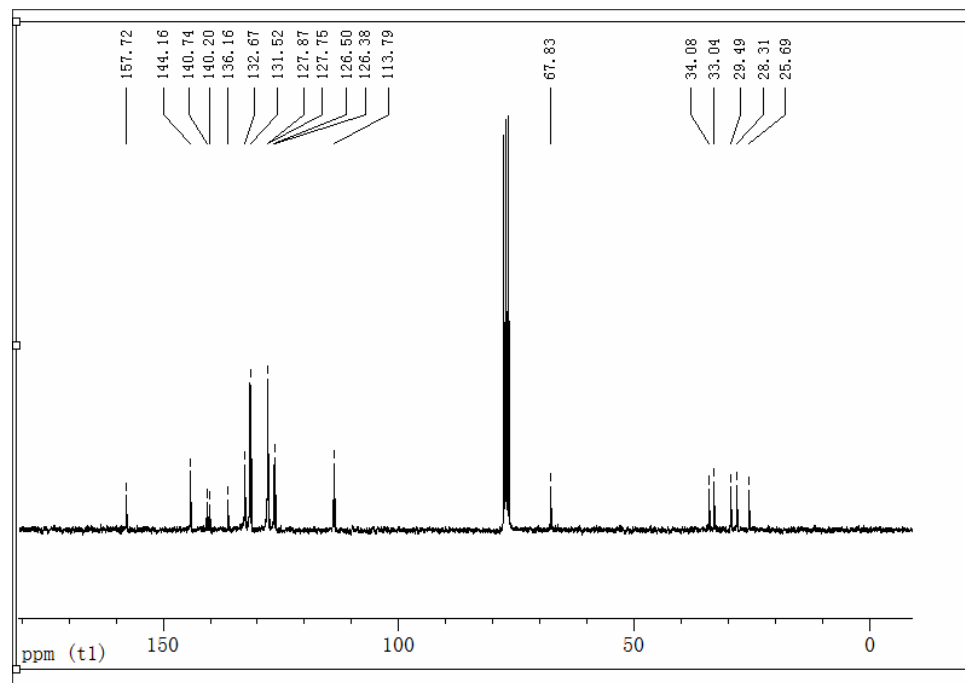


3. EHBr

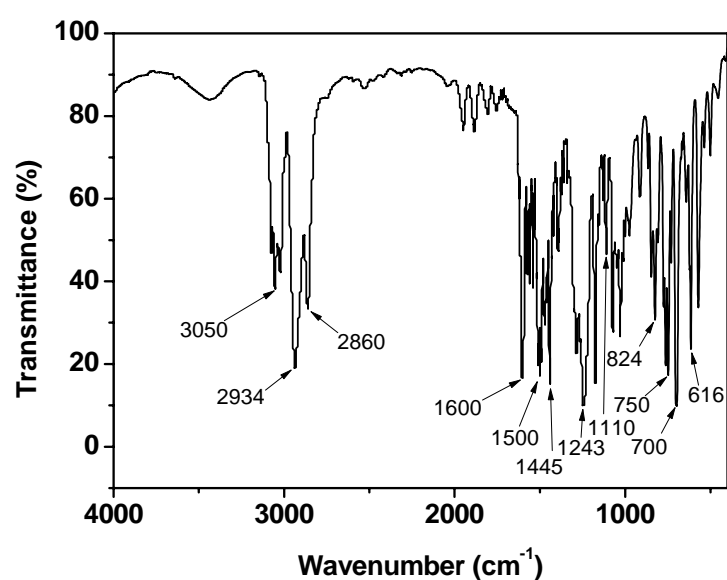
^1H NMR



^{13}C NMR



FT-IR

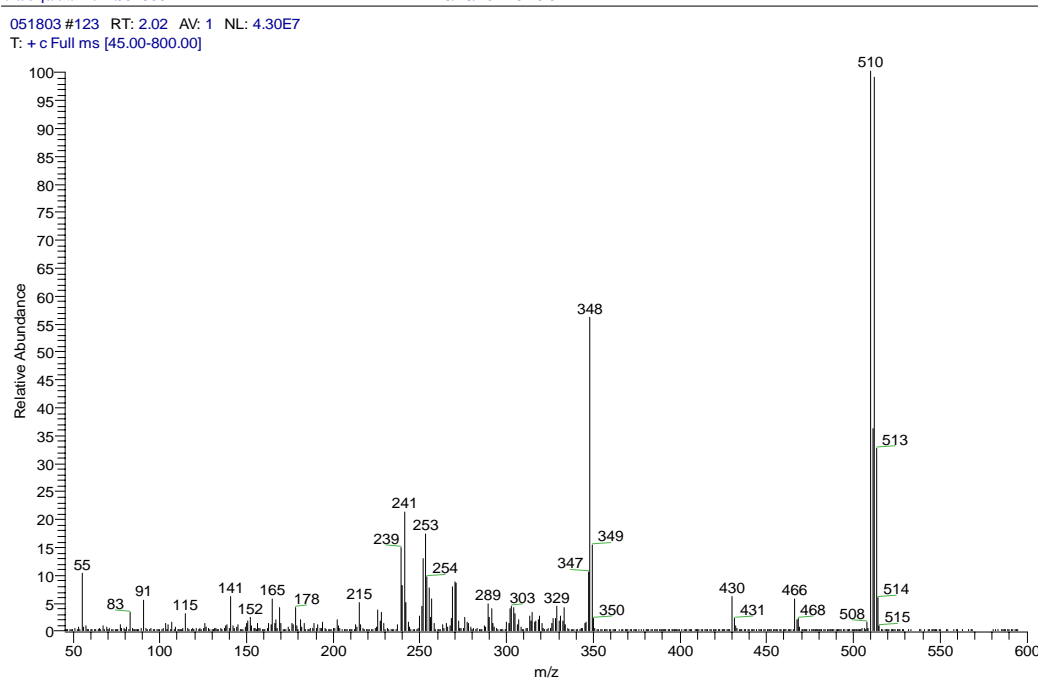


EI-MS

Instrument:DSQ(Thermo)
Ionization Method:EI
d:\dsq\data\lr\12\051803

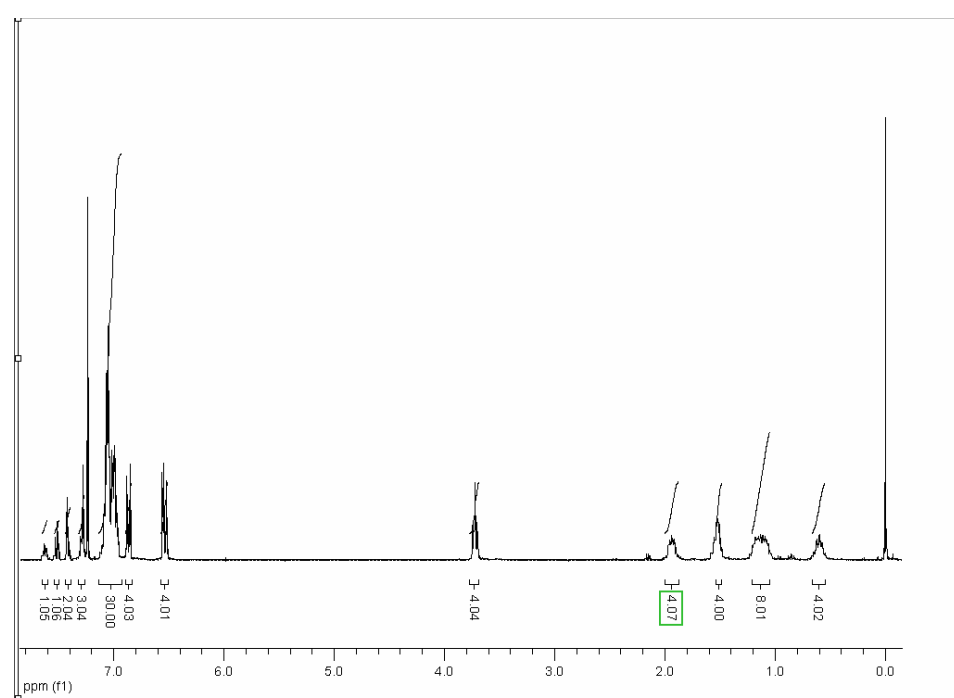
5/18/2012 3:46:57 PM

EHBr

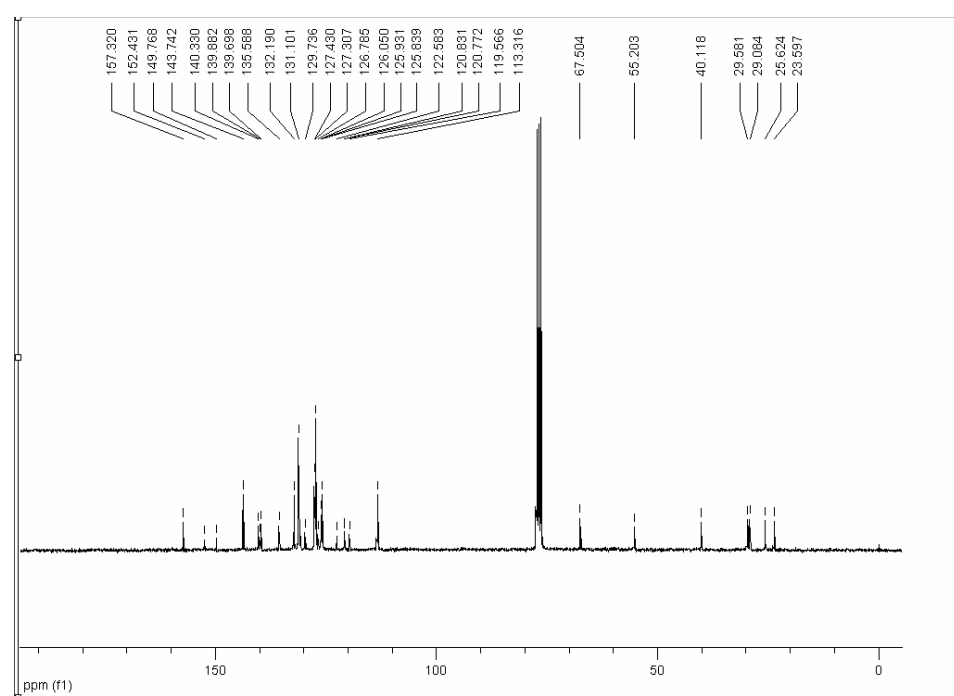


4. FHE₂Br

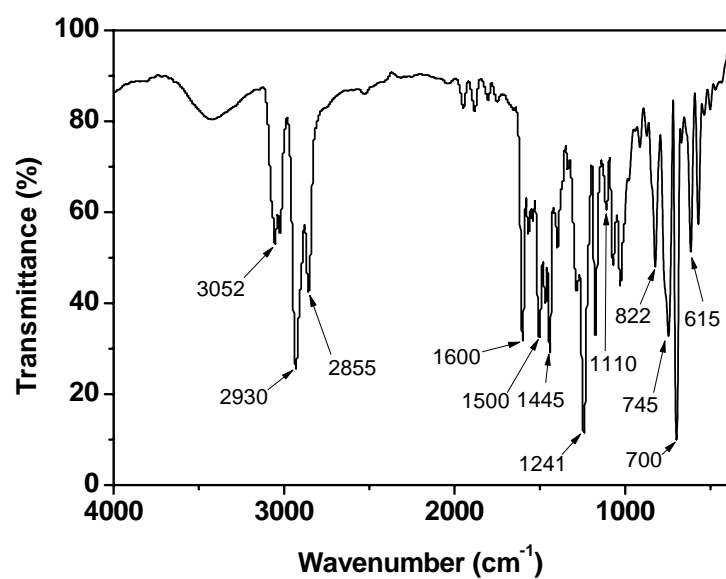
¹H NMR



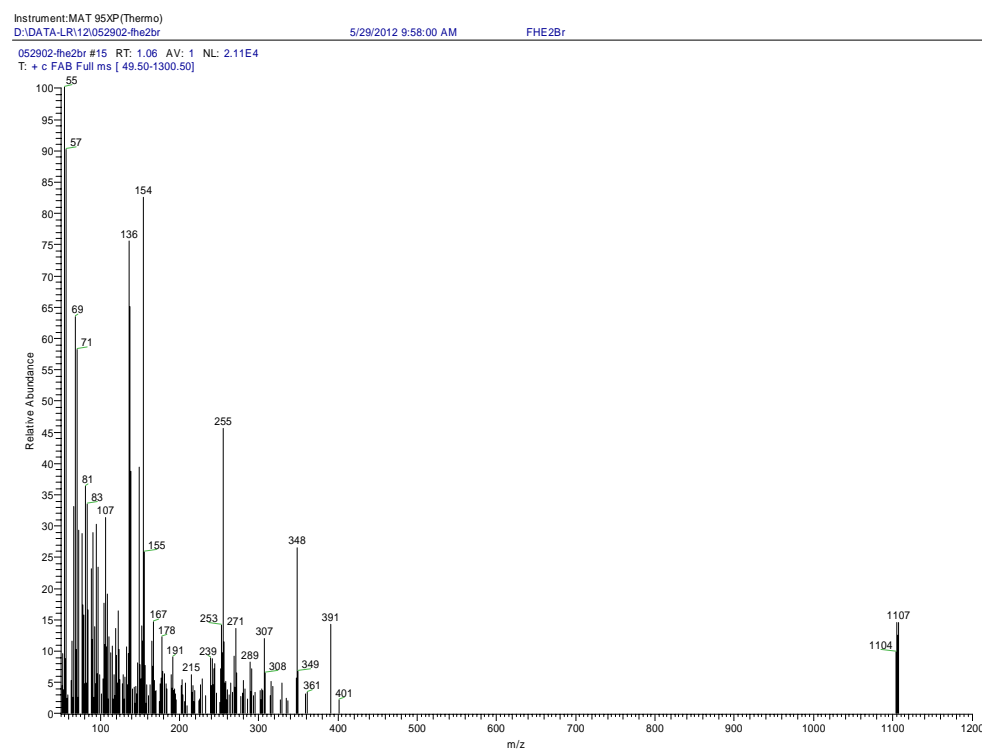
¹³C NMR



FT-IR

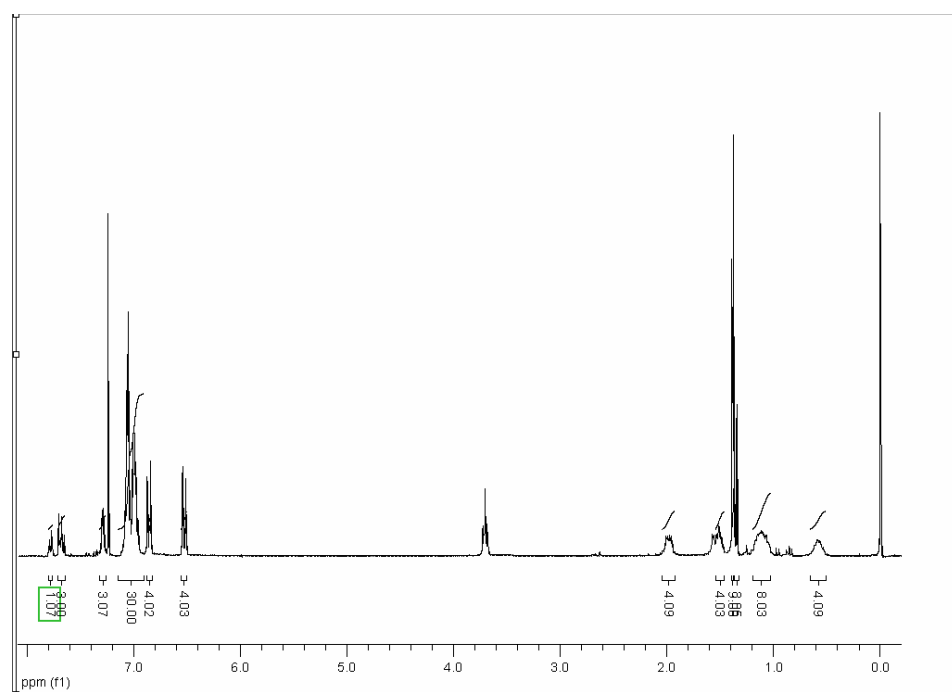


EI-MS

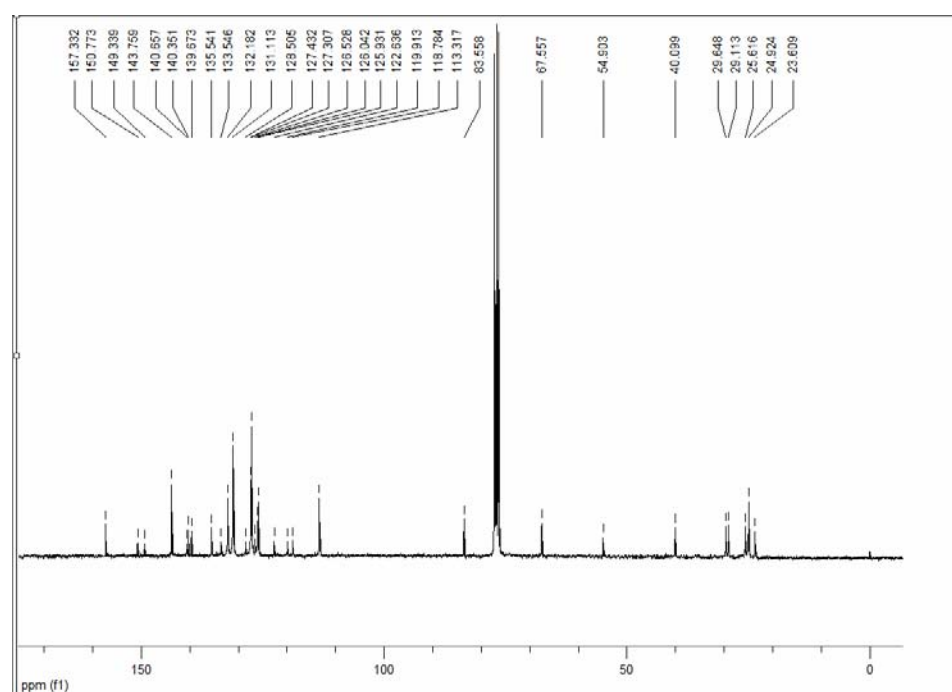


5. FHE₂B

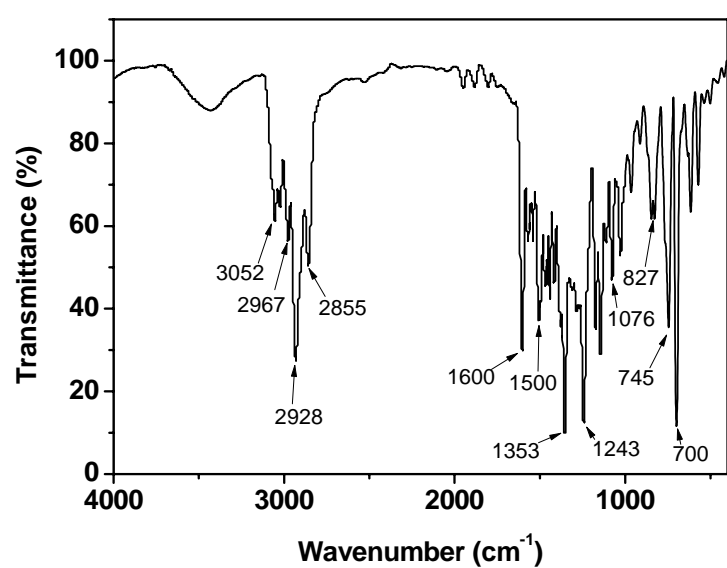
¹H NMR



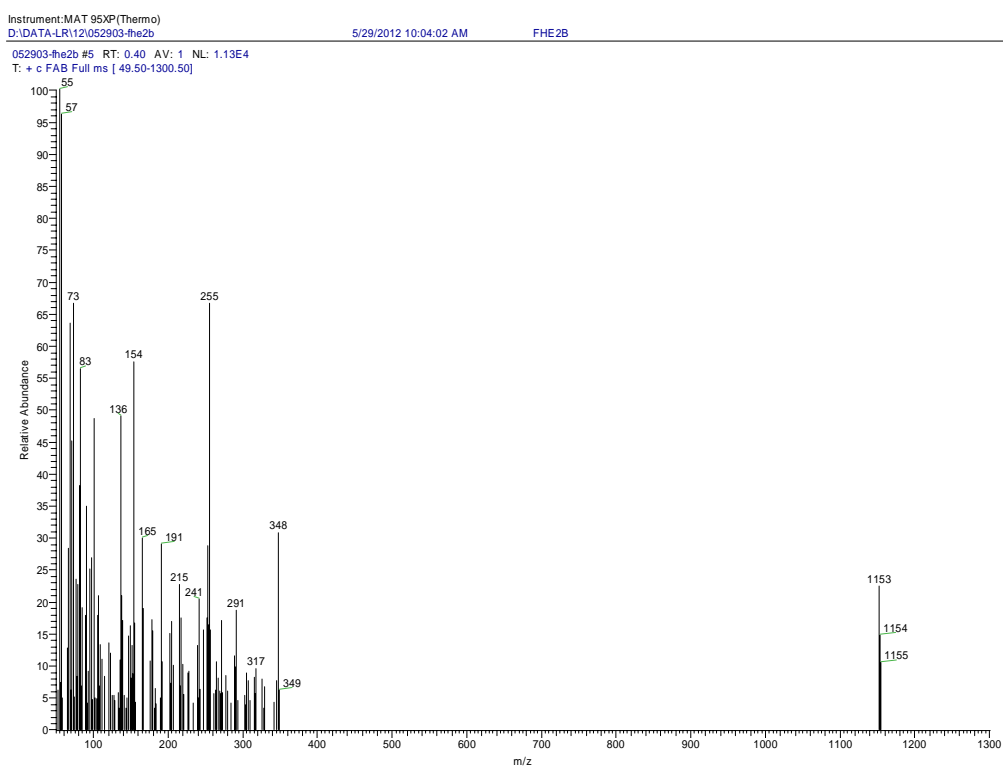
¹³C NMR



FT-IR

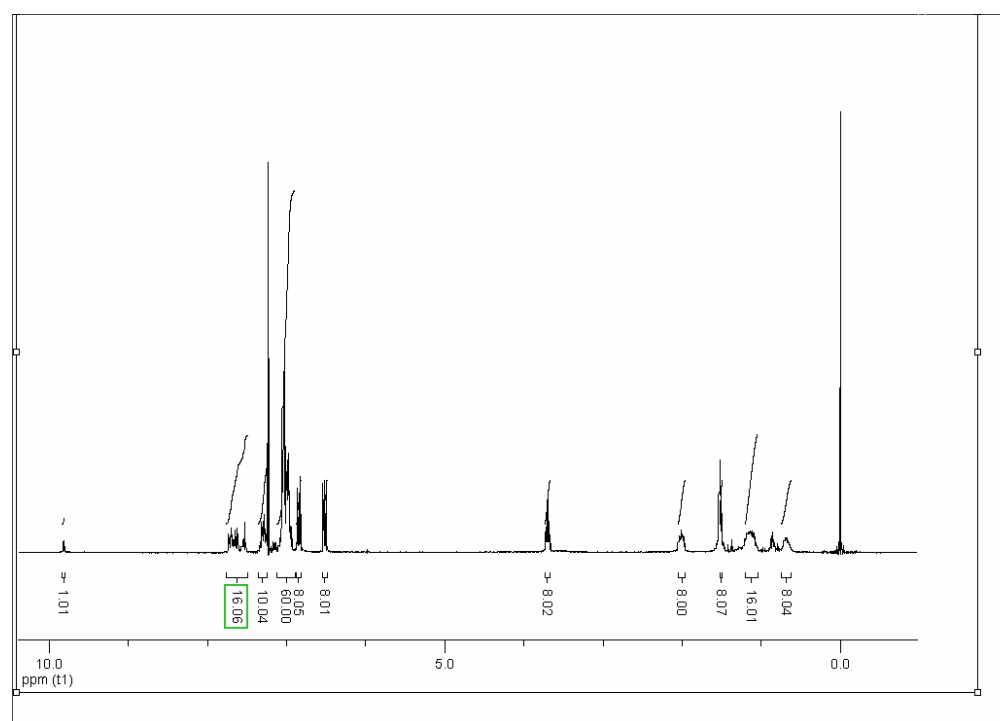


EI-MS

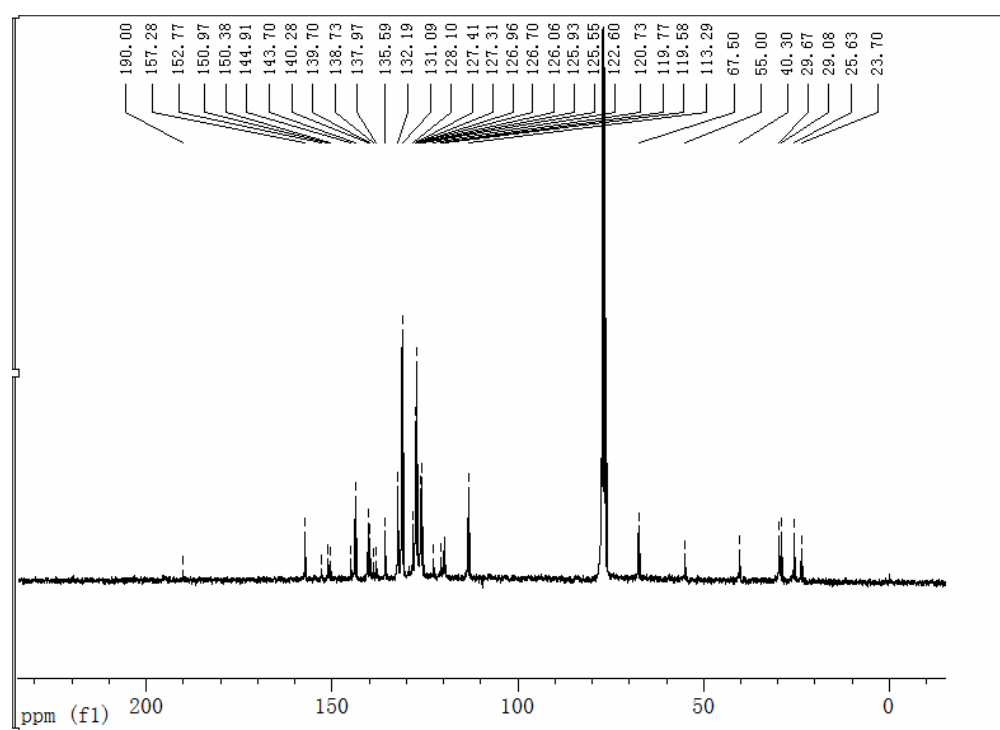


6. $\text{AF}_2\text{H}_4\text{E}_4$

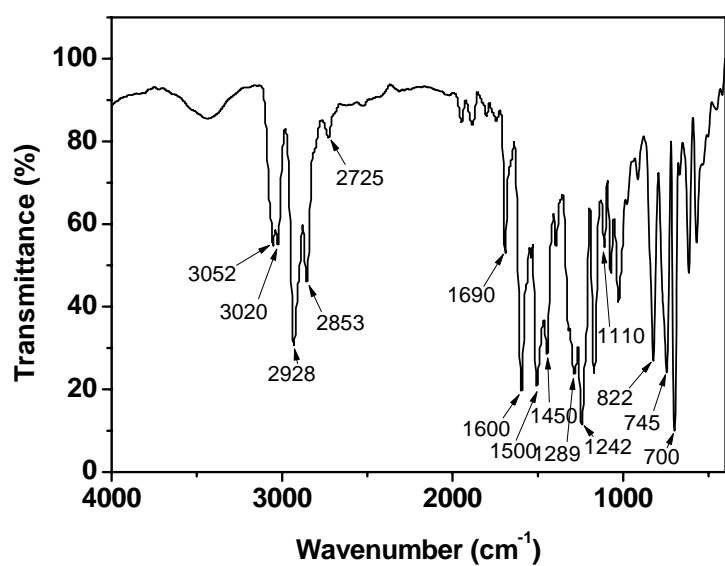
^1H NMR



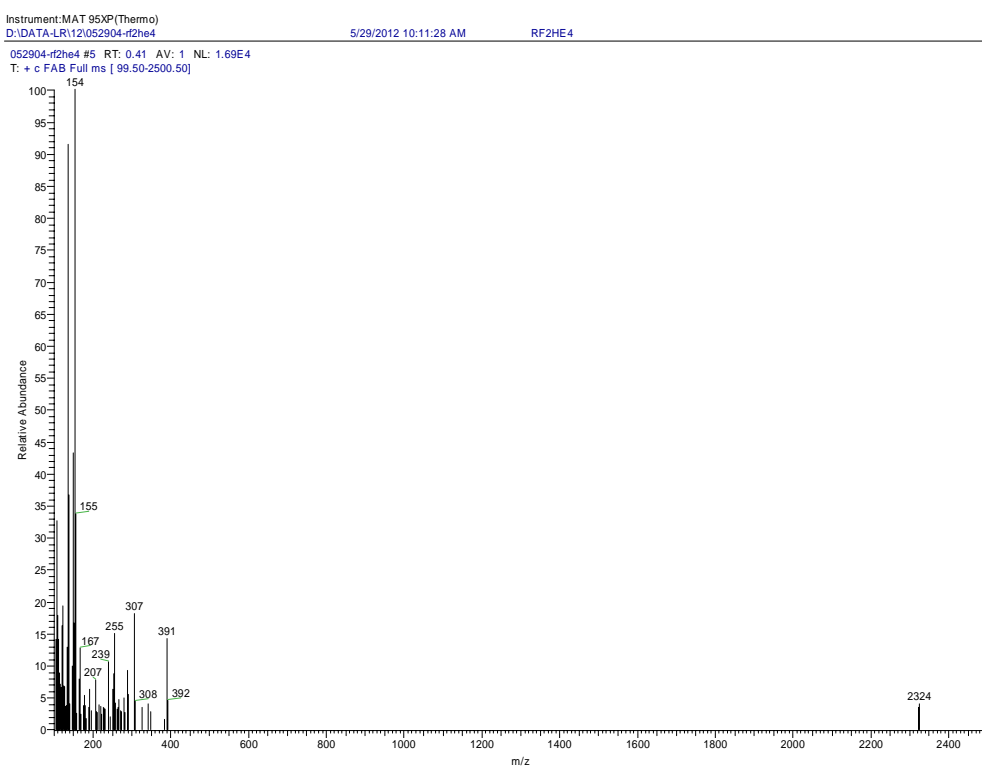
^{13}C NMR



FT-IR

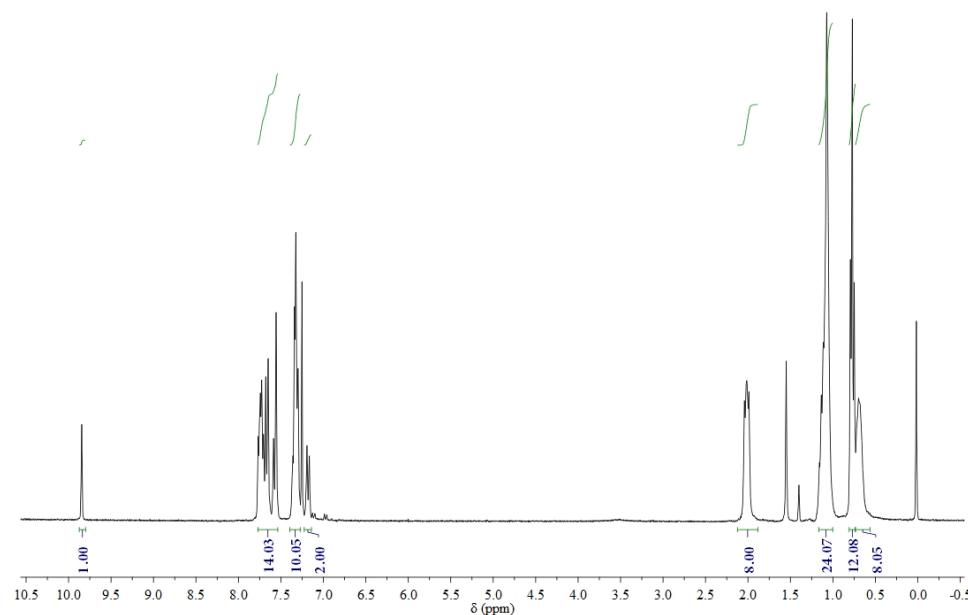


EI-MS

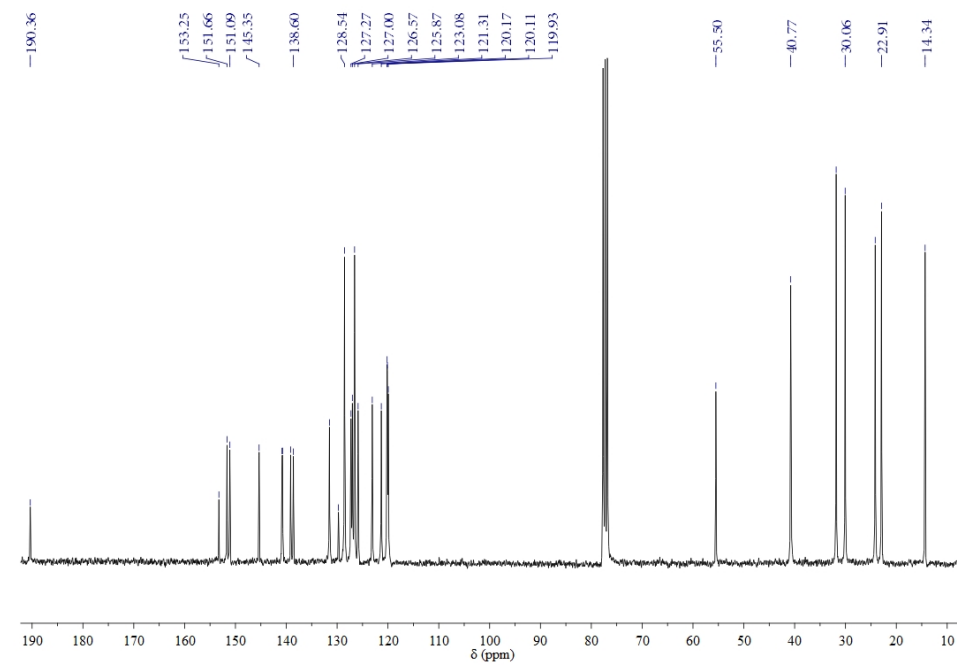


7. AF_2H_4

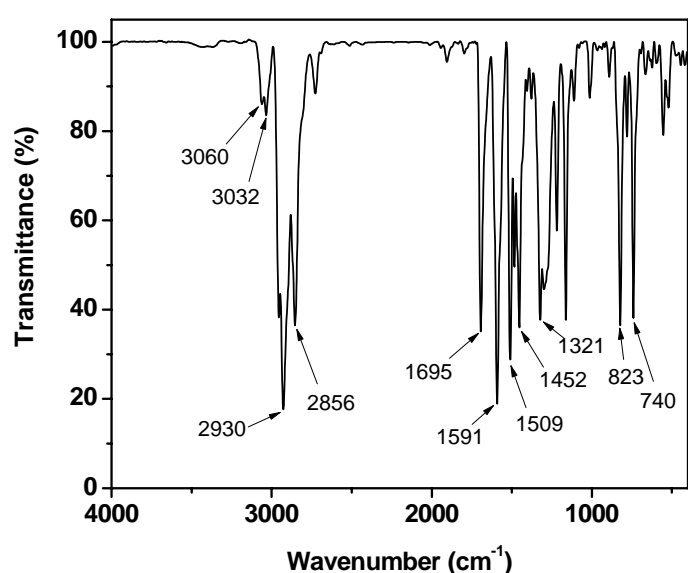
^1H NMR



^{13}C NMR



FT-IR



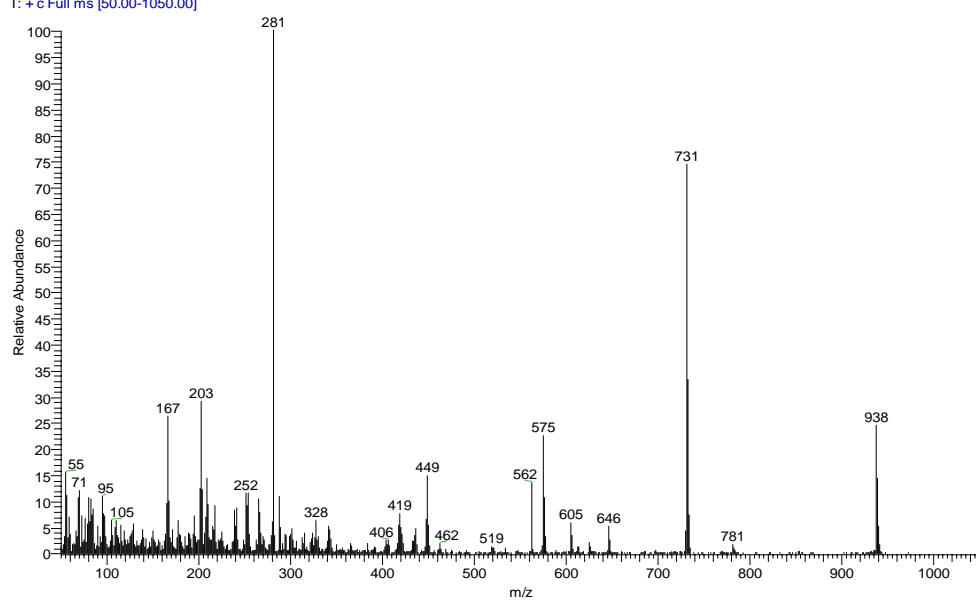
EI-MS

Instrument:DSQ(Thermo)
Ionization Method:EI
D:\DSQ\DATA-LR13\012202

1/22/2013 11:26:45 AM

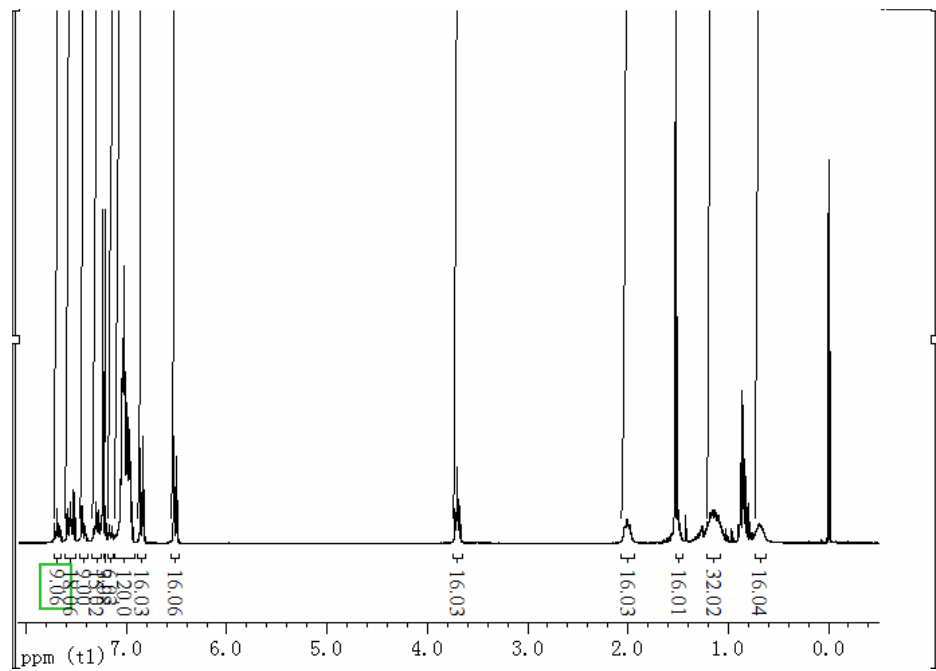
AF2H4

012202 #119 RT: 4.02 AV: 1 NL: 2.08E5
T: + c Full ms [50.00-1050.00]

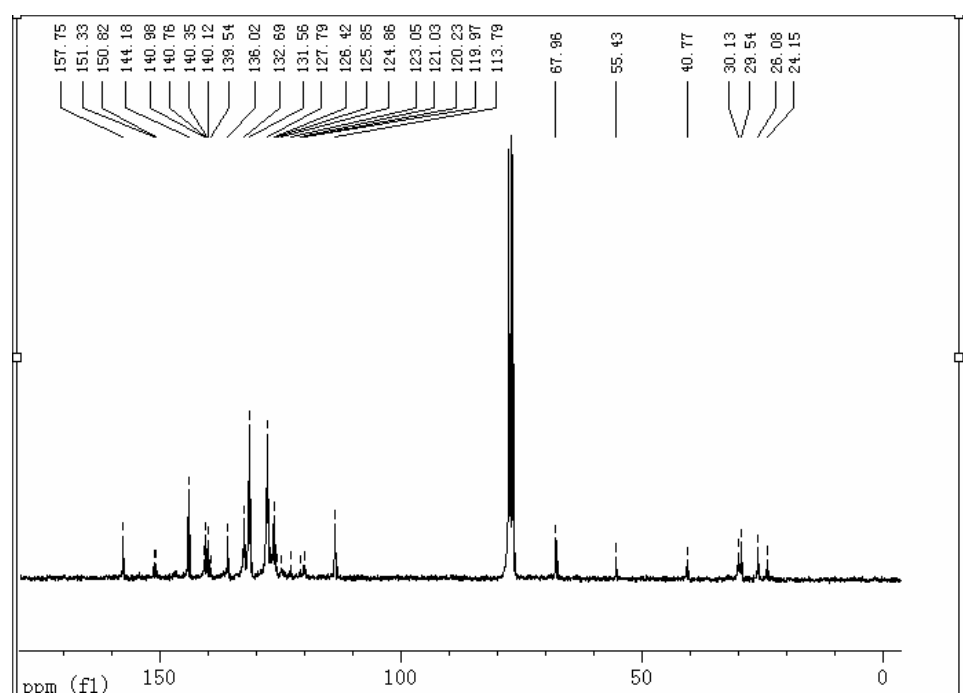


8. $\text{PA}_2\text{F}_4\text{H}_8\text{E}_8$

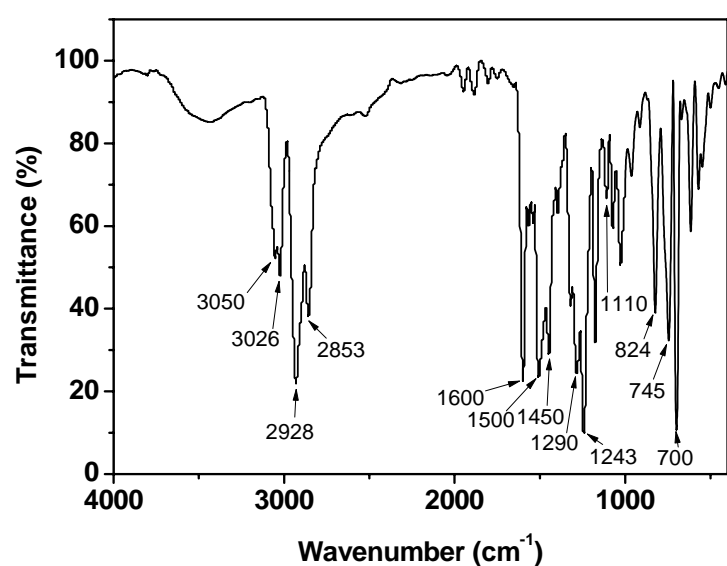
^1H NMR



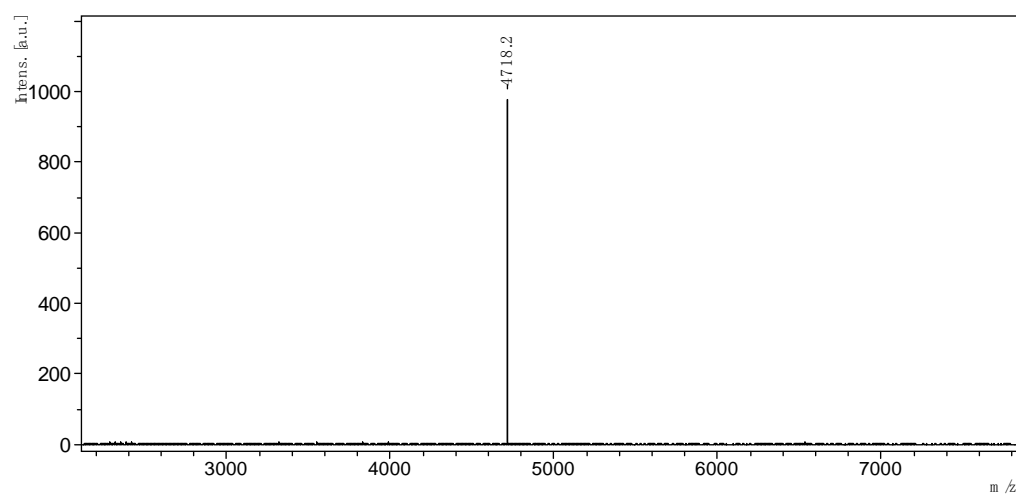
^{13}C NMR



FT-IR

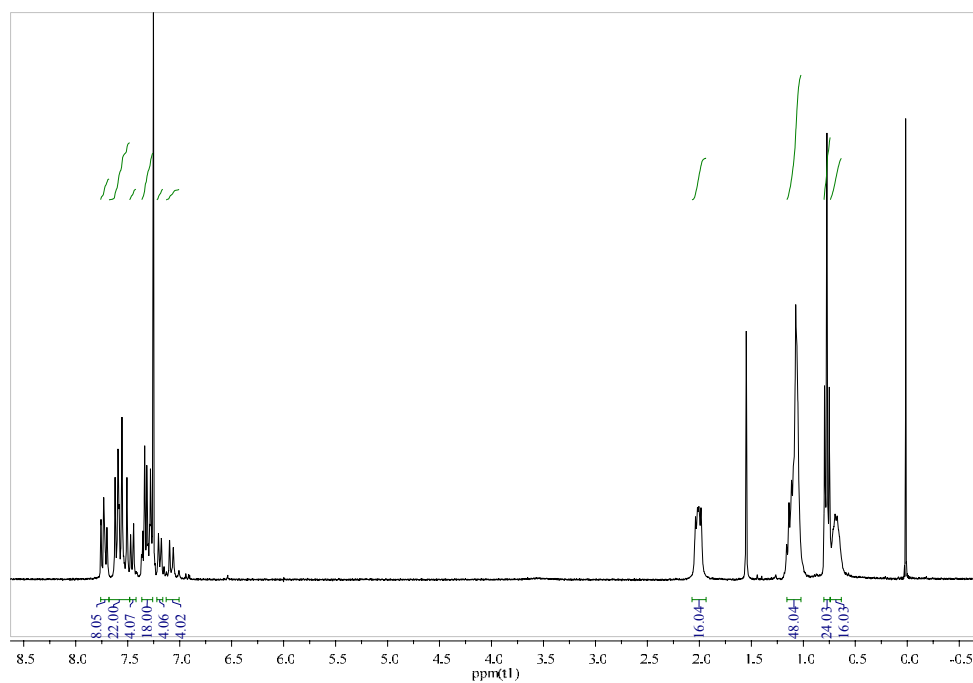


MALDI-TOF-MS

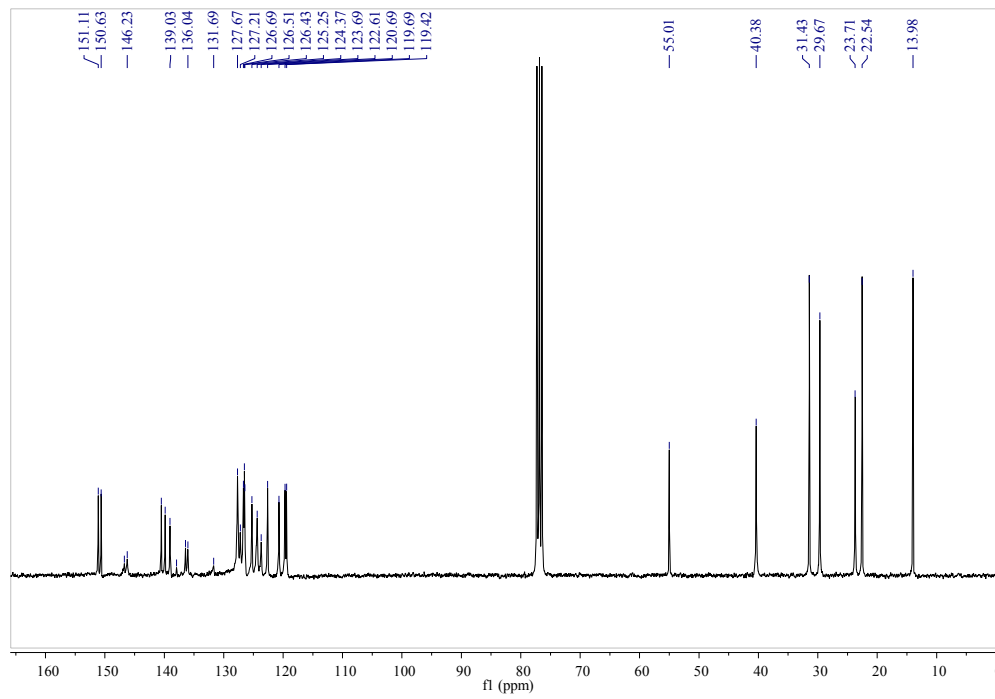


9. PA₂F₄H₈

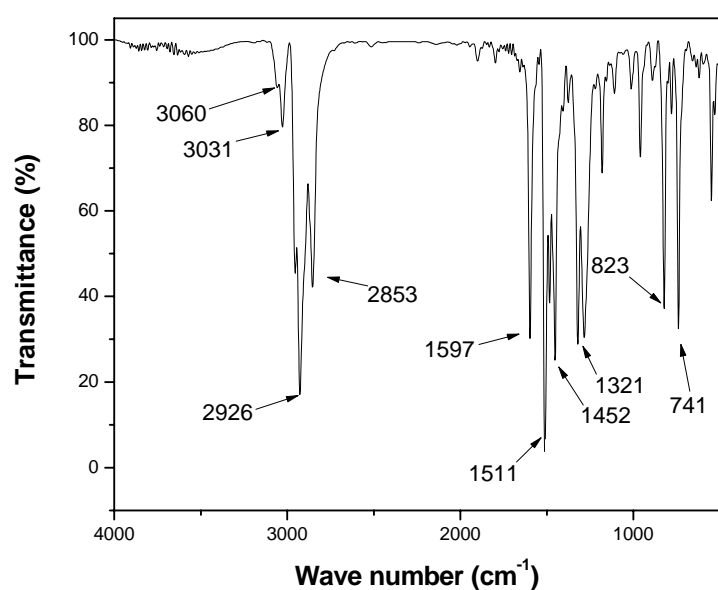
¹H NMR



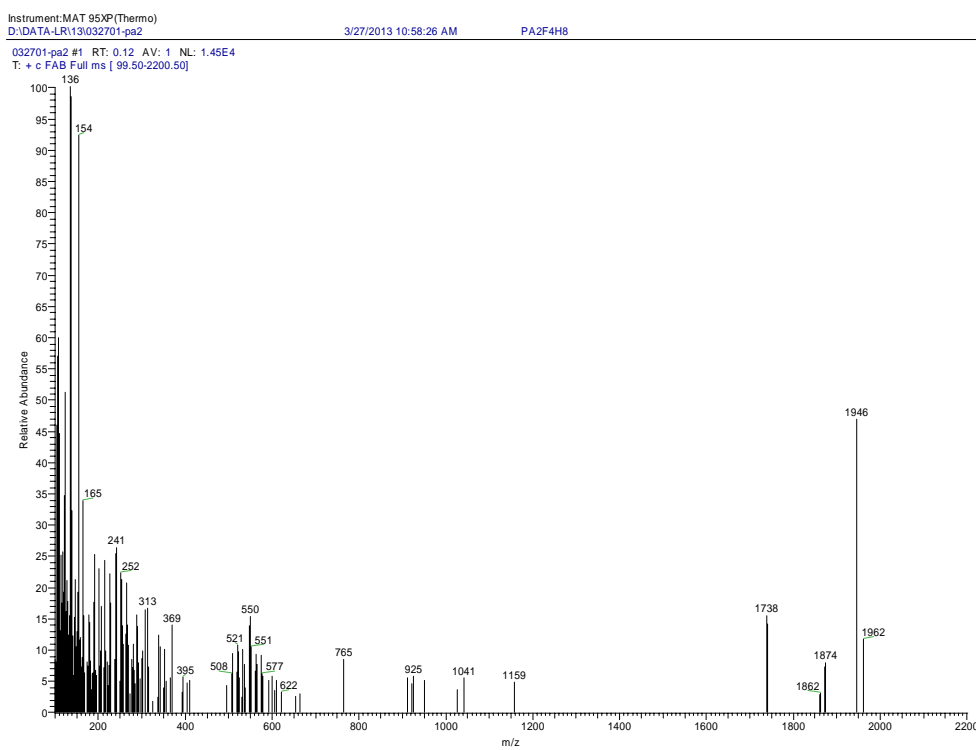
¹³C NMR



FT-IR

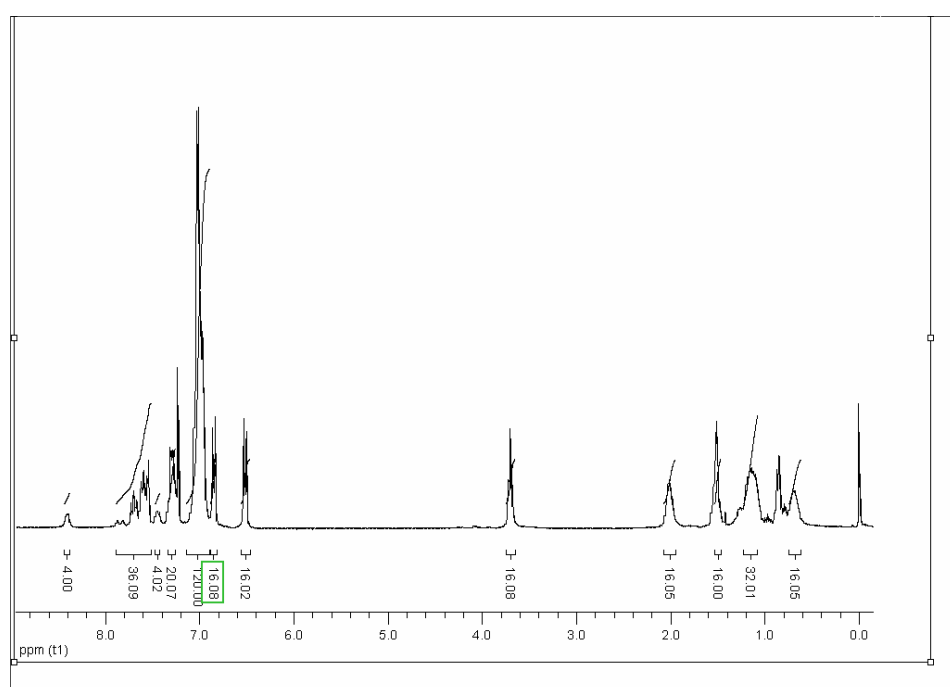


FAB-MS

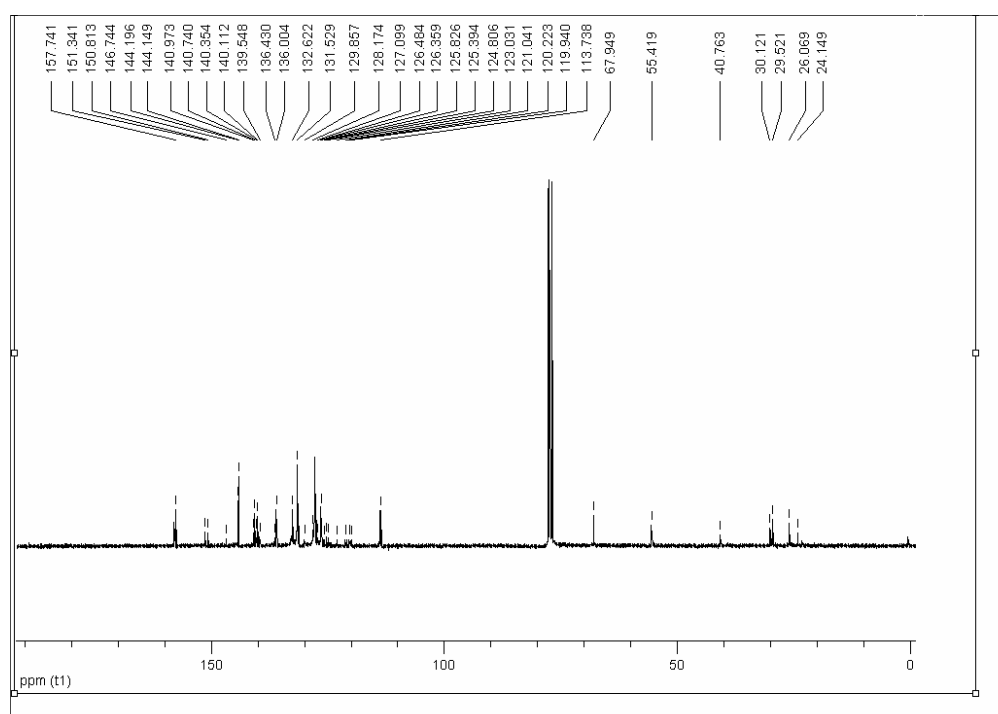


10. AnA₂F₄H₈E₈

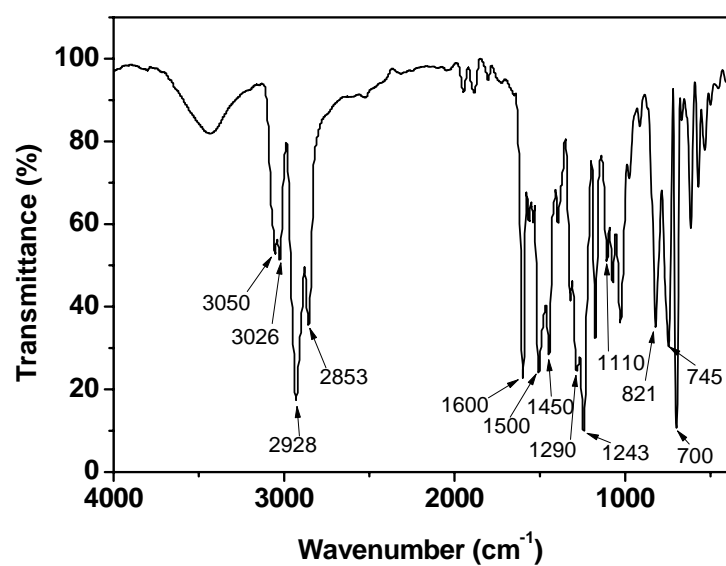
¹H NMR



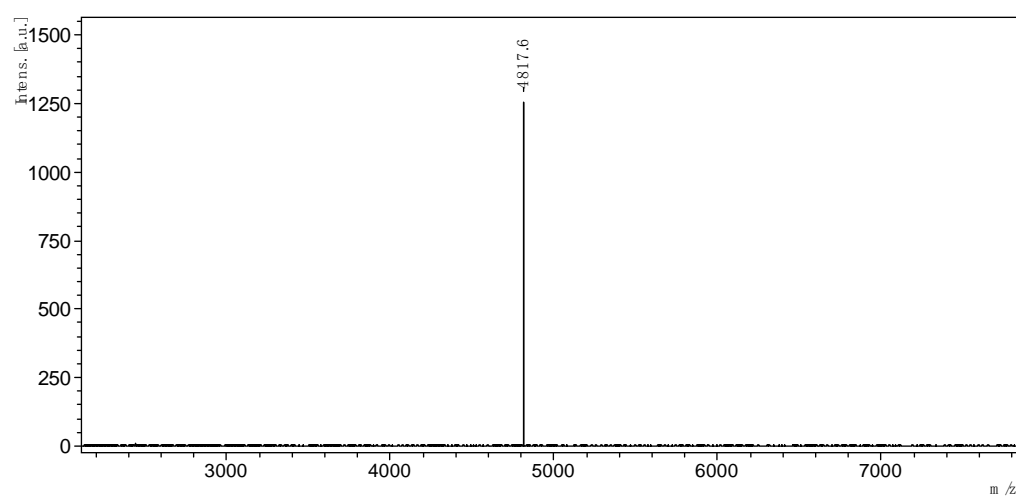
¹³C NMR



FT-IR

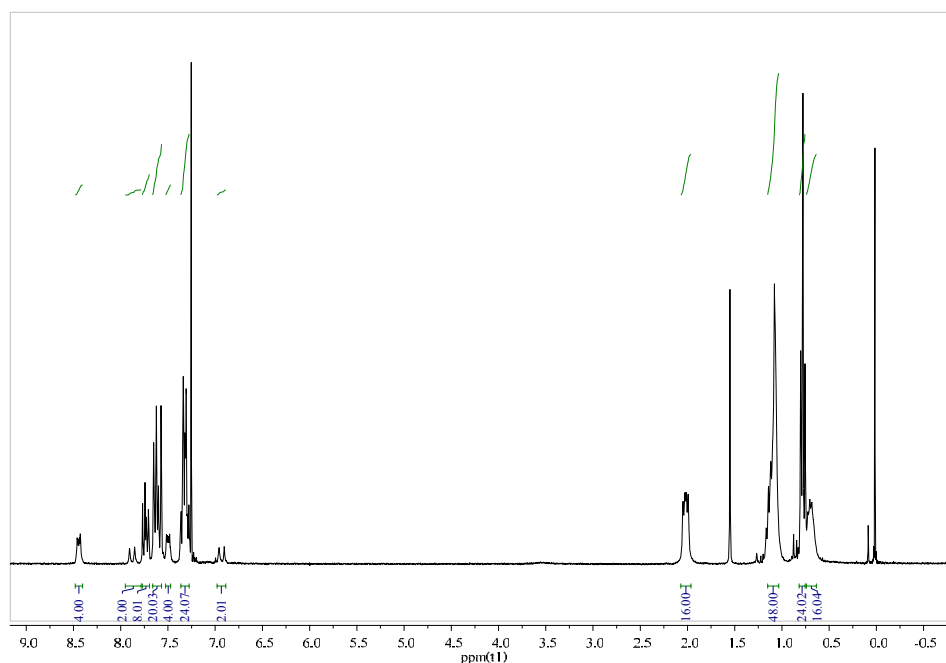


MALDI-TOF-MS

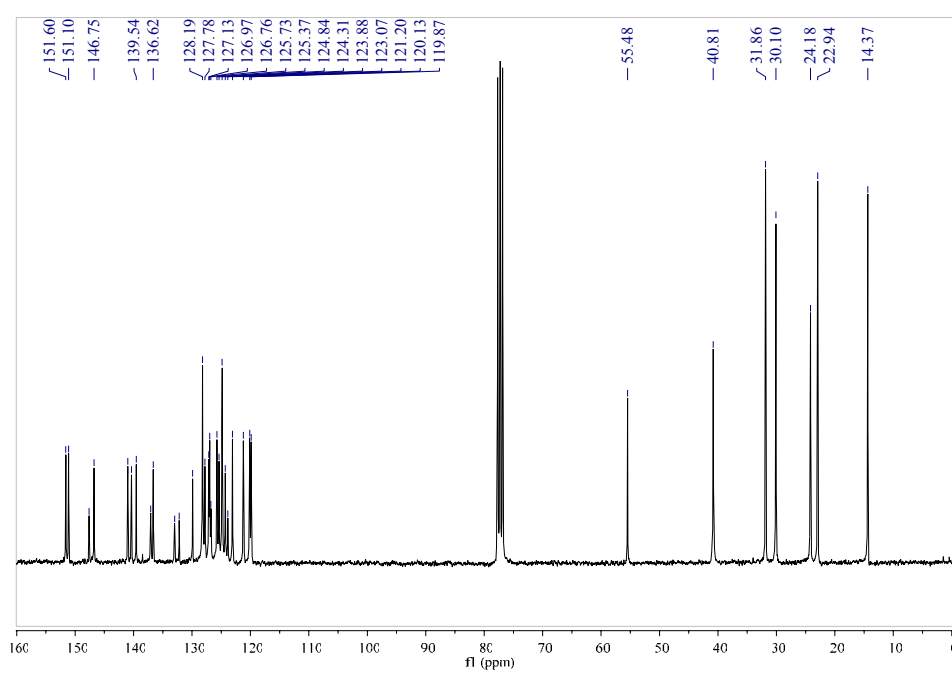


11. $\text{AnA}_2\text{F}_4\text{H}_8$

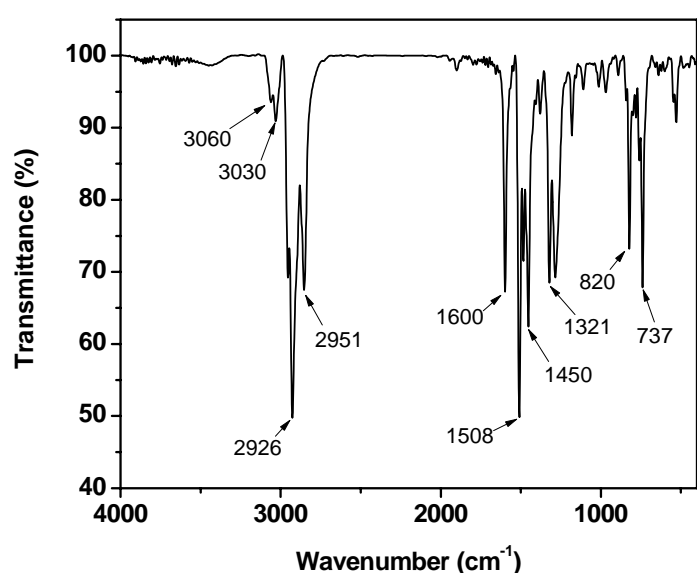
^1H NMR



^{13}C NMR



FT-RI



MALDI-TOF-MS

